



**Calhoun: The NPS Institutional Archive**  
**DSpace Repository**

---

Theses and Dissertations

1. Thesis and Dissertation Collection, all items

---

1990-06

## Comparison of slotline characteristics

Seo, Yong Seok

Monterey, California: Naval Postgraduate School

---

<https://hdl.handle.net/10945/34829>

---

Copyright is reserved by the copyright owner.

*Downloaded from NPS Archive: Calhoun*



Calhoun is the Naval Postgraduate School's public access digital repository for research materials and institutional publications created by the NPS community. Calhoun is named for Professor of Mathematics Guy K. Calhoun, NPS's first appointed -- and published -- scholarly author.

**Dudley Knox Library / Naval Postgraduate School**  
**411 Dyer Road / 1 University Circle**  
**Monterey, California USA 93943**

<http://www.nps.edu/library>

AD-A236 685



2

# NAVAL POSTGRADUATE SCHOOL Monterey, California



DTIC  
ELECTE  
JUN 06 1991  
S B D

## THESIS

COMPARISON OF SLOTLINE CHARACTERISTICS

by

Yong Seok Seo

June 1990

Thesis Advisor:

R. Janaswamy

Approved for public release; distribution is unlimited

91 6 4 038

91-01166



Unclassified

security classification of this page

REPORT DOCUMENTATION PAGE

1a Report Security Classification <b>Unclassified</b>		1b Restrictive Markings	
2a Security Classification Authority		3 Distribution Availability of Report <b>Approved for public release; distribution is unlimited.</b>	
2b Declassification Downgrading Schedule		5 Monitoring Organization Report Number(s)	
4 Performing Organization Report Number(s)		7a Name of Monitoring Organization <b>Naval Postgraduate School</b>	
6a Name of Performing Organization <b>Naval Postgraduate School</b>	6b Office Symbol <i>(if applicable)</i> <b>52</b>	7b Address <i>(city, state, and ZIP code)</i> <b>Monterey, CA 93943-5000</b>	
6c Address <i>(city, state, and ZIP code)</i> <b>Monterey, CA 93943-5000</b>		9 Procurement Instrument Identification Number	
8a Name of Funding Sponsoring Organization	8b Office Symbol <i>(if applicable)</i>	10 Source of Funding Numbers	
8c Address <i>(city, state, and ZIP code)</i>		Program Element No	Project No
		Task No	Work Unit Accession No
11 Title <i>(include security classification)</i> <b>COMPARISON OF SLOTLINE CHARACTERISTICS</b>			
12 Personal Author(s) <b>Seo , Yong Seok</b>			
13a Type of Report <b>Master's Thesis</b>	13b Time Covered From To	14 Date of Report <i>(year, month, day)</i> <b>June 1990</b>	15 Page Count <b>53</b>
16 Supplementary Notation <b>The views expressed in this thesis are those of the author and do not reflect the official policy or position of the Department of Defense or the U.S. Government.</b>			
17 Cosati Codes		18 Subject Terms <i>(continue on reverse if necessary and identify by block number)</i>	
Field	Group	Characteristics of single-sided slotline, bilateral slotline, and asymmetric slotline.	
19 Abstract <i>(continue on reverse if necessary and identify by block number)</i> <p>The slot width required for conventional slotlines is very narrow when etched on low dielectric constant substrates. This poses fabrication difficulties and discourages the use of slotlines on these substrates. However, the slotline is finding increased applications in slot antennas. In order to feed the slot antennas, alternate structures must be found that relax the fabrication difficulties. Two such new structures are the bilateral slotline and the asymmetric slotline [Refs. 6,7]. In this thesis, design data was developed and comparison was made between the various slotlines with regards to the substrate parameters and the slot width. Use was made of computer codes already developed for these structures.</p>			
20 Distribution Availability of Abstract <input checked="" type="checkbox"/> unclassified unlimited <input type="checkbox"/> same as report <input type="checkbox"/> DTIC users		21 Abstract Security Classification <b>Unclassified</b>	
22a Name of Responsible Individual <b>Ramakrishna Janaswamy</b>		22b Telephone <i>(include Area code)</i> <b>(408) 646-3217</b>	22c Office Symbol <b>54Ss</b>

Approved for public release; distribution is unlimited.

Comparison of Slotline Characteristics

by

Seo , Yong Seok  
Major , Korean Army  
B.S., Army Academy, 1981

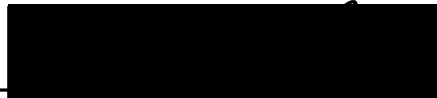
Submitted in partial fulfillment of the  
requirements for the degree of

MASTER OF SCIENCE IN ELECTRICAL AND COMPUTER ENGINEERING

from the

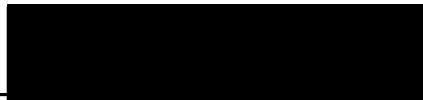
NAVAL POSTGRADUATE SCHOOL  
June 1990

Author:



Seo , Yong Seok

Approved by:



Ramakrishna Janaswamy, Thesis Advisor



Jeffrey B. Knorr, Second Reader



John P. Powers, Chairman,  
Department of Electrical and Computer Engineering

### ABSTRACT.

The slot width required for conventional slotlines is very narrow when etched on low dielectric constant substrates. This poses fabrication difficulties and discourages the use of slotlines on these substrates. However, the slotline is finding increased applications in slot antennas. In order to feed the slot antennas, alternate structures must be found that relax the fabrication difficulties. Two such new structures are the bilateral slotline and the asymmetric slotline [Refs. 6,7]. In this thesis, design data was developed and comparison was made between the various slotlines with regards to the substrate parameters and the slot width. Use was made of computer codes already developed for these structures.



Accession For	
NTIS GRA&I	<input checked="" type="checkbox"/>
DTIC TAB	<input type="checkbox"/>
Unannounced	<input type="checkbox"/>
Justification	
By	
Distribution/	
Availability Codes	
Dist	Avail and/or Special
A-1	

## TABLE OF CONTENTS

I. INTRODUCTION .....	1
II. SINGLE-SIDED SLOTLINE .....	5
A. HIGH PERMITTIVITY SUBSTRATES .....	6
B. LOW PERMITTIVITY SUBSTRATES .....	8
III. BILATERAL SLOTLINE .....	18
IV. ASYMMETRIC SLOTLINE .....	27
V. CONCLUSION .....	36
APPENDIX A. THE PROGRAM OF THE SINGLE-SIDED SLOTLINE	37
LIST OF REFERENCES .....	41
INITIAL DISTRIBUTION LIST .....	43

## LIST OF FIGURES

Figure 1. Tapered Slot Antenna. ....	3
Figure 2. The Cross-section of the Three Slotlines. ....	4
Figure 3. $\epsilon_{eff}$ and $Z_o$ versus $\frac{d}{\lambda_o} \sqrt{\epsilon_r - 1}$ , for $\epsilon_r = 2.22$ . ....	13
Figure 4. $\epsilon_{eff}$ and $Z_o$ versus $\frac{d}{\lambda_o} \sqrt{\epsilon_r - 1}$ , for $\epsilon_r = 3.0$ . ....	14
Figure 5. $\epsilon_{eff}$ and $Z_o$ versus $\frac{d}{\lambda_o} \sqrt{\epsilon_r - 1}$ , for $\epsilon_r = 6.0$ . ....	15
Figure 6. $\epsilon_{eff}$ and $Z_o$ versus $\frac{d}{\lambda_o} \sqrt{\epsilon_r - 1}$ , for $\epsilon_r = 10.0$ . ....	16
Figure 7. $\epsilon_{eff}$ and $Z_o$ versus $\frac{d}{\lambda_o} \sqrt{\epsilon_r - 1}$ , for $\epsilon_r = 12.8$ . ....	17
Figure 8. Microstrip-Slotline Transition. ....	21
Figure 9. $\epsilon_{eff}$ and $Z_o$ versus $\frac{d}{\lambda_o} \sqrt{\epsilon_r - 1}$ , for $\epsilon_r = 2.22$ . ....	22
Figure 10. $\epsilon_{eff}$ and $Z_o$ versus $\frac{d}{\lambda_o} \sqrt{\epsilon_r - 1}$ , for $\epsilon_r = 3.0$ . ....	23
Figure 11. $\epsilon_{eff}$ and $Z_o$ versus $\frac{d}{\lambda_o} \sqrt{\epsilon_r - 1}$ , for $\epsilon_r = 6.0$ . ....	24
Figure 12. $\epsilon_{eff}$ and $Z_o$ versus $\frac{d}{\lambda_o} \sqrt{\epsilon_r - 1}$ , for $\epsilon_r = 10.0$ . ....	25
Figure 13. $\epsilon_{eff}$ and $Z_o$ versus $\frac{d}{\lambda_o} \sqrt{\epsilon_r - 1}$ , for $\epsilon_r = 12.8$ . ....	26
Figure 14. Microstrip line-Asymmetric Slotline Transition. ....	30
Figure 15. $\epsilon_{eff}$ and $Z_o$ versus $\frac{d}{\lambda_o} \sqrt{\epsilon_r - 1}$ , for $\epsilon_r = 2.22$ . ....	31
Figure 16. $\epsilon_{eff}$ and $Z_o$ versus $\frac{d}{\lambda_o} \sqrt{\epsilon_r - 1}$ , for $\epsilon_r = 3.0$ . ....	32

Figure 17. $\epsilon_{eff}$ and $Z_o$ versus $\frac{d}{\lambda_o} \sqrt{\epsilon_r - 1}$ , for $\epsilon_r = 6.0$ . . . . .	33
Figure 18. $\epsilon_{eff}$ and $Z_o$ versus $\frac{d}{\lambda_o} \sqrt{\epsilon_r - 1}$ , for $\epsilon_r = 10.0$ . . . . .	34
Figure 19. $\epsilon_{eff}$ and $Z_o$ versus $\frac{d}{\lambda_o} \sqrt{\epsilon_r - 1}$ , for $\epsilon_r = 12.8$ . . . . .	35



## ACKNOWLEDGEMENTS

I really thank to my Holy God who saved me and loves me endlessly, and I wish to express my sincere appreciation to my thesis advisor, Professor Ramakrishna Janaswamy. He was a consistent wellspring of sound advice, technical competence, professional assistance, and moral support. Without his assistance, this thesis could not have been undertaken.

I am also thankful to Professor J. B. Knorr and my senior officer Hwang Jungsub who provided help with their excellent knowledge and warm hearts. I would also like to thank to my wife, Kyehwa, and my daughter, Jimin, for their support and love away from home during our time in the United States. And finally I thank to my mother and to my father who is in Heaven.

## I. INTRODUCTION

The planar tapered slot antenna shown in Fig. 1 is increasingly being used these days as a phased array element in microwave and millimeter wave subsystems [Refs. 1, 2]. The antenna is essentially a flared slotline designed to produce a symmetrical end-fire beam. The radiation pattern characteristics depend on the substrate parameters as well as on the taper geometry [Ref. 3]. The dielectric constant of the substrate is generally low ( $\epsilon_r < 9.8$ ) and the substrate is electrically thin. Some of the important characteristics of the antenna are its wide bandwidth, high gain, and compatibility with integrated circuits. Arrays of the antenna elements configured to give a multiple-beam have been used in millimeter wave imaging systems [Ref. 2]. Detector diodes may be connected directly across the feed gap in such applications. However, in a majority of applications one would like feed these antennas by means of standard printed transmission lines such as microstrip line or stripline. A transition between the input feed line and the slotline needs to be designed for proper coupling of power. Several microstrip-to-slotline transitions have been reported in the literature [Ref. 4]. In all these transitions, the width of the feeding slotline becomes very narrow leading to fabrication difficulty. The situation gets worse for lower  $\epsilon_r$  substrates. This can be partially overcome by using alternative substrate metallizations for the antenna and the associated feed slotline. In this thesis, we compare the propagation characteristics of three different slotlines used in the design of the tapered slot antenna.

Figure 2 shows the cross-section of the three slotlines. Antennas designed with all of these configurations have been shown to be good radiating elements [Ref. 5].

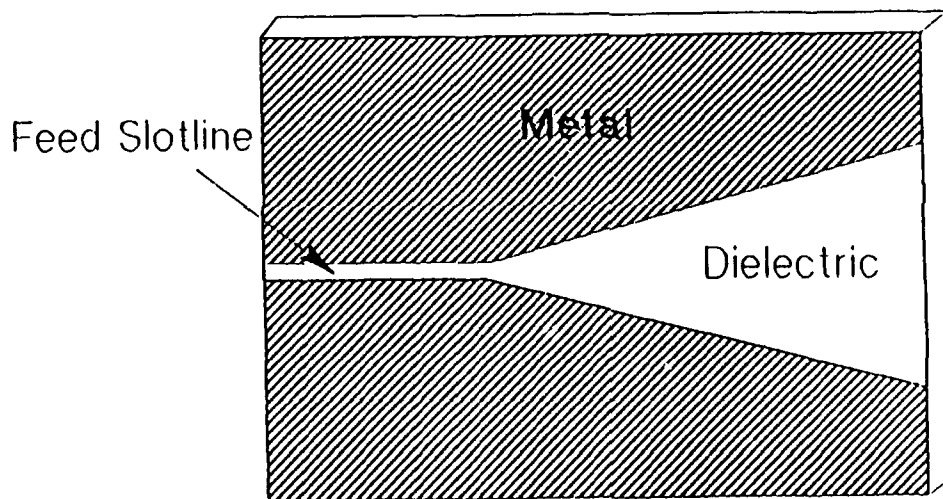
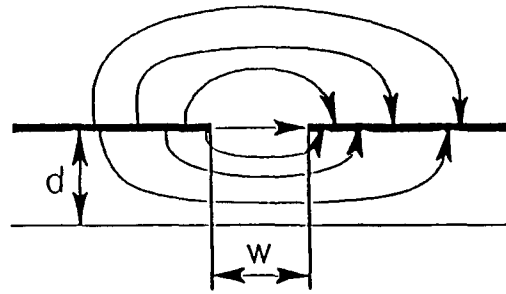
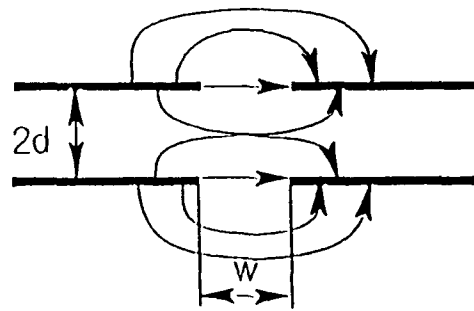


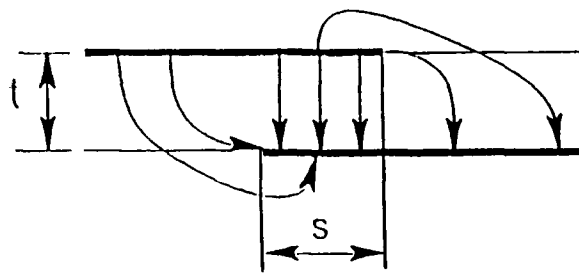
Figure 1. Taperd Slot Antenna.



(a) Single-Sided Slotline



(b) Bilateral Slotline



(c) Asymmetric Slotline

Figure 2. The Cross-section of the Three Slotlines.

## II. SINGLE-SIDED SLOTLINE

Slotline is an alternative transmission structure proposed for use in MICs by Cohn in 1968. The basic slotline shown in Fig. 2 (a) consists of a dielectric substrate of dielectric constant  $\epsilon_r$  with a narrow slotwidth  $w$  etched in the metallization on one of the surfaces of the dielectric substrate of thickness  $d$ . The other surface of the substrate is without any metallization. The geometry is planar and well-suited for its use in microwave integrated circuits. We call such a transmission line the *single-sided slotline*.

Slotlines can be included in microstrip circuits by etching the slotline circuit in the ground plane of the substrate for microstrip circuits. This type of hybrid combination allows flexibility in the design of microwave circuits and has led to some new types of circuits, such as hybrid branchline directional couplers. Also, some of the circuit elements which cannot easily be achieved in microstrip configuration can be incorporated in the slotline part of the circuit. These, for example, could be short circuits, high impedance lines or series stubs. Figure 8 shows a typical microstrip line-to-slotline transition.

In the single-sided slotline, the mode of propagation is non-TEM and there is no low frequency cut-off for the mode. Design formulas are provided for the effective dielectric constant  $\epsilon_{eff}$  and the characteristic impedance  $Z_o$ . The effective dielectric constant is the inverse of square of the normalized slot wavelength  $\lambda_s/\lambda_o$ . The characteristic impedance is based on the power-voltage definition:  $Z_o = |V|^2/P$ , where  $V$  is the r m s transverse voltage across the slot and  $P$  is the

average power carried by the line. Data are provided for  $\epsilon_r = 2.22, 3.0, 6.0, 10.0,$  and 12.8 for  $0.01 \leq \frac{d}{\lambda_o} \sqrt{\epsilon_r - 1} \leq 0.25$  over the range  $0.0015 \leq w/\lambda_o \leq 1.0,$  and  $0.006 \leq d/\lambda_o \leq 0.06$  in [Ref. 4].

Since the slotline is non-TEM in nature, its characteristic impedance is not defined uniquely. It has been shown in [Ref. 9] that to match to a 50 ohm microstrip line, one needs a 70-75 ohm slotline with its characteristic impedance defined as above. We shall take examples of five substrates:  $\epsilon_r = 2.22, d = 50$  mils;  $\epsilon_r = 3.0, d = 50$  mils;  $\epsilon_r = 6.0, d = 50$  mils;  $\epsilon_r = 10.0, d = 50$  mils; and  $\epsilon_r = 12.8, d = 50$  mils and compare the widths needed to realize a 75 ohm slotline at a frequency of 9 GHz.

#### A. HIGH PERMITTIVITY SUBSTRATES

By high permittivity substrates, we mean substrates having a dielectric constant  $\epsilon_r$  in excess of 9.8. Empirical formulas have been developed in [Ref. 4] for the normalized slot wavelength  $\lambda_s/\lambda_o$  and the slot characteristic impedance  $Z_o$ . The expressions for high permittivity substrates have an accuracy of about 2 percent for the following sets of parameters:

$$9.8 \leq \epsilon_r \leq 20$$

$$0.02 \leq w/d \leq 1.0, \text{ and}$$

$$0.01 \leq d/\lambda_o \leq (d/\lambda_o)_c,$$

where  $(d/\lambda_o)_c$  is equal to the cut-off value for the  $TE_o$  surface-wave mode on an ungrounded dielectric slab. The expressions are

1) For  $0.02 \leq w/d < 0.2$

$$\lambda_s/\lambda_o = 0.923 - 0.448 \log \epsilon_r + 0.2w/d \quad (1.1)$$

$$- (0.29w/d + 0.047) \log(d/\lambda_o \times 10^2)$$

$$Z_o = 72.62 - 35.19 \log \epsilon_r + 50 \frac{(w/d - 0.02)(w/d - 0.1)}{w/d} \quad (1.2)$$

$$+ \log(w/d \times 10^2)[44.28 - 19.58 \log \epsilon_r]$$

$$- [0.32 \log \epsilon_r - 0.11 + w/d(1.07 \log \epsilon_r + 1.44)]$$

$$\times (11.4 - 6.07 \log \epsilon_r - d/\lambda_o \times 10^2)^2$$

2) For  $0.2 \leq w/d \leq 1.0$

$$\lambda_s/\lambda_o = 0.987 - 0.483 \log \epsilon_r + w/d(0.111 - 0.0022\epsilon_r) \quad (1.3)$$

$$- (0.121 + 0.094w/d - 0.0032\epsilon_r) \log(d/\lambda_o \times 10^2)$$

$$Z_o = 113.19 - 53.55 \log \epsilon_r + 1.25w/d(114.59 - 51.88 \log \epsilon_r) \quad (1.4)$$

$$+ 20(w/d - 0.2)(1 - w/d)$$



$$\begin{aligned}
& - [0.15 + 0.23 \log \epsilon_r + w/d(-0.79 + 2.07 \log \epsilon_r)] \\
& \times [10.25 - 5 \log \epsilon_r + w/d(2.1 - 1.42 \log \epsilon_r) - d/\lambda_o \times 10^2]^2
\end{aligned}$$

Slotline characteristics using the above formulas are plotted in Figs. 6 and 7. To realize a 75 ohm slotline on a 50 mil substrate, we obtain from Figs. 6 and 7,  $w/d = 0.214$ ,  $w = 10.7$  mils for  $\epsilon_r = 10.0$ , and  $w/d = 0.2906$ ,  $w = 14.53$  mils for  $\epsilon_r = 12.8$ . As we see, the values of  $w$ , the slot width, increase as the value of substrate permittivity increases.

## B. LOW PERMITTIVITY SUBSTRATES

Low permittivity substrates are characterized by  $\epsilon_r$  less than 9.8. Empirical formulas for low permittivity substrates have been developed for the normalized slot wavelength  $\lambda_s/\lambda_o$  and the slot characteristic impedance  $Z_o$  in [Ref. 5] and are given below. These formulas have been obtained by least-square curve-fitting the computed data. In each case, the average of the absolute percentage error "av" and the maximum percentage error "max," observed in a systematic sample of 120 data points, are given.

The following formulas are all valid within  $0.006 \leq d/\lambda_o \leq 0.06$ .

- 1)  $2.22 \leq \epsilon_r \leq 3.8$

a)  $0.0015 \leq w/\lambda_o \leq 0.075$

$$\lambda_s/\lambda_o = 1.045 - 0.365 \ln \epsilon_r + \frac{6.3(w/d)\epsilon_r^{0.945}}{(238.64 + 100w/d)} \quad (1.5)$$

$$- \left[ 0.148 - \frac{8.81(\epsilon_r + 0.95)}{100\epsilon_r} \right] \ln(d/\lambda_o)$$

av = 0.37%, max = 2.2% (at one point)

$$Z_o = 60 + 3.69 \sin \left[ \frac{(\epsilon_r - 2.22)\pi}{2.36} \right] + 133.5 \ln(10\epsilon_r) \sqrt{w/\lambda_o} \quad (1.6)$$

$$+ 2.81[1 - 0.011\epsilon_r(4.48 + \ln \epsilon_r)](w/d) \ln(100d/\lambda_o)$$

$$+ 131.1(1.028 - \ln \epsilon_r) \sqrt{d/\lambda_o}$$

$$+ 12.48(1 + 0.18 \ln \epsilon_r) \frac{w/d}{\sqrt{\epsilon_r - 2.06 + 0.85(w/d)^2}}$$

av = 0.67%, max = 2.7% (at one point)

b)  $0.075 \leq w/\lambda_o \leq 1.0$

$$\lambda_s/\lambda_o = 1.194 - 0.24 \ln \epsilon_r - \frac{0.621\epsilon_r^{0.835}(w/\lambda_o)^{0.48}}{(1.344 + w/d)} \quad (1.7)$$

$$- 0.0617 \left[ 1.91 - \frac{(\epsilon_r + 2)}{\epsilon_r} \right] \ln(d/\lambda_o)$$

av = 0.69%, max = - 2.6% (at two points, for  $w/\lambda_o > 0.8$ )

$$Z_o = 133 + 10.34(\epsilon_r - 1.8)^2 + 2.87[2.96 + (\epsilon_r - 1.582)^2] \quad (1.8)$$

$$\times \{w/d + 2.32\epsilon_r - 0.56\}$$

$$\times \{(32.5 - 6.67\epsilon_r)(100d/\lambda_o)^2 - 1\}^{1/2}$$

$$- (684.45d/\lambda_o)(\epsilon_r + 1.35)^2$$

$$+ 13.23[(\epsilon_r - 1.722)w/\lambda_o]^2$$

av = 1.9%, |max| = 5.4%, (at three points, for  $w/\lambda_o > 0.8$ )

2)  $3.8 \leq \epsilon_r \leq 9.8$

a)  $0.0015 \leq w/\lambda_o \leq 0.075$

$$\lambda_s/\lambda_o = 0.9217 - 0.277 \ln \epsilon_r + 0.0322(w/d) \left[ \frac{\epsilon_r}{(w/d + 0.435)} \right]^{1/2} \quad (1.9)$$

$$- 0.01 \ln(d/\lambda_o) \left[ 4.6 - \frac{3.65}{\epsilon_r^2 \sqrt{w/\lambda_o} (9.06 - 100w/\lambda_o)} \right]$$

av = 0.6%, |max| = 3% (at three points, occurs for  $w/d > 1$ ,  $\epsilon_r > 6.0$ )

$$Z_o = 73.6 - 2.15\epsilon_r + (638.9 - 31.37\epsilon_r)(w/\lambda_o)^{0.6} \quad (1.10)$$

$$+ (36.23\sqrt{\epsilon_r^2 + 41} - 225) \frac{w/d}{(w/d + 0.876\epsilon_r - 2)}$$

$$+ 0.51(\epsilon_r + 2.12)(w/d) \ln(100d/\lambda_o)$$

$$- 0.753\epsilon_r(d/\lambda_o)/\sqrt{w/\lambda_o}$$

av = 1.58%, max = 5.4%(at three points, occurs for  $w/d > 1.67$ )

b)  $0.075 \leq w/\lambda_o \leq 1.0$

$$\lambda_s/\lambda_o = 1.05 - 0.04\epsilon_r + 1.411 \times 10^{-2}(\epsilon_r - 1.421) \quad (1.11)$$

$$\times \ln\{w/d - 2.012(1 - 0.146\epsilon_r)\}$$

$$+ 0.111(1 - 0.366\epsilon_r)\sqrt{w/\lambda_o}$$

$$+ 0.139(1 + 0.52\epsilon_r \ln(14.7 - \epsilon_r))(d/\lambda_o) \ln(d/\lambda_o)$$

av = 0.75%, |max| = 3.2%(at two points, occurs for  $w/\lambda_o = 0.075$ ,  $d/\lambda_o > 0.03$ )

$$Z_o = 120.75 - 3.74\epsilon_r + 50[\tan^{-1}(2\epsilon_r) - 0.8] \quad (1.12)$$

$$\times (w/d)^{[1.11 + (0.132(\epsilon_r - 27.7)/(100d/\lambda_o + 5))]}$$

$$\begin{aligned} & \times \ln [100d/\lambda_o + \sqrt{(100d/\lambda_o)^2 + 1}] \\ & + 14.21(1 - 0.458\epsilon_r)(100d/\lambda_o + 5.1 \ln \epsilon_r - 13.1) \\ & \times (w/\lambda_o + 0.33)^2 \end{aligned}$$

$$av = 2.0\%, |\max| = 5.8\% (\text{at two points, occurs for } w/\lambda_o < 0.1)$$

Curves corresponding to  $\epsilon_r = 2.22, 3.0,$  and  $6.0$  are plotted in Figs. 3 - 5. To realize a 75 ohm slotline on a 50 mil substrate as we did in the case of high permittivity substrates, we require  $w/d = 0.0852$  and  $w = 4.26$  mils for  $\epsilon_r = 6.0$  in Fig. 5. But for  $\epsilon_r = 2.22$  and  $\epsilon_r = 3.0$ , we see that  $w < 2$  mils to obtain 75 ohms. The values of characteristic impedance we obtain when  $\epsilon_r = 2.22$  and  $\epsilon_r = 3.0$  are over 75 ohms for practically realizable slot widths.

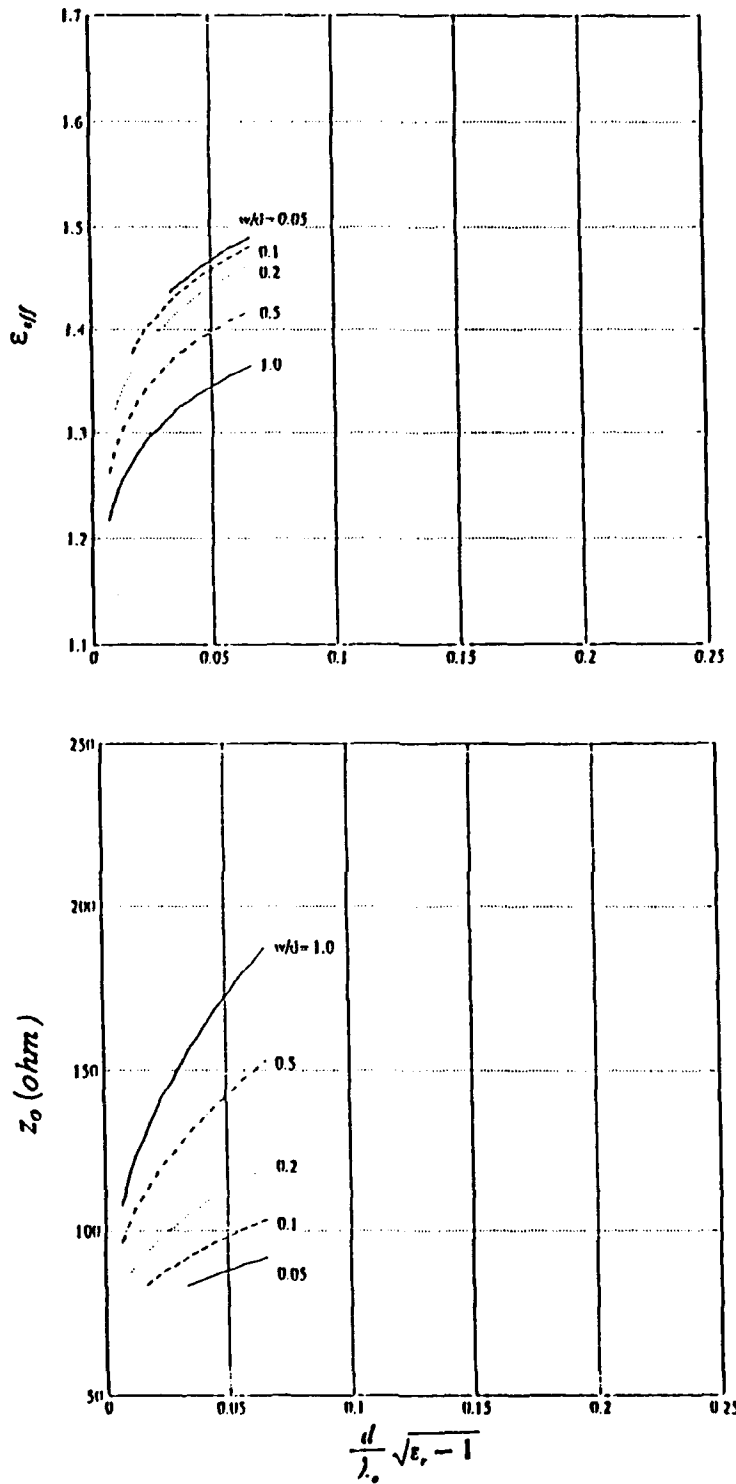


Figure 3.  $\epsilon_{eff}$  and  $Z_0$  versus  $\frac{d}{\lambda_0} \sqrt{\epsilon_r - 1}$ , for  $\epsilon_r = 2.22$ .

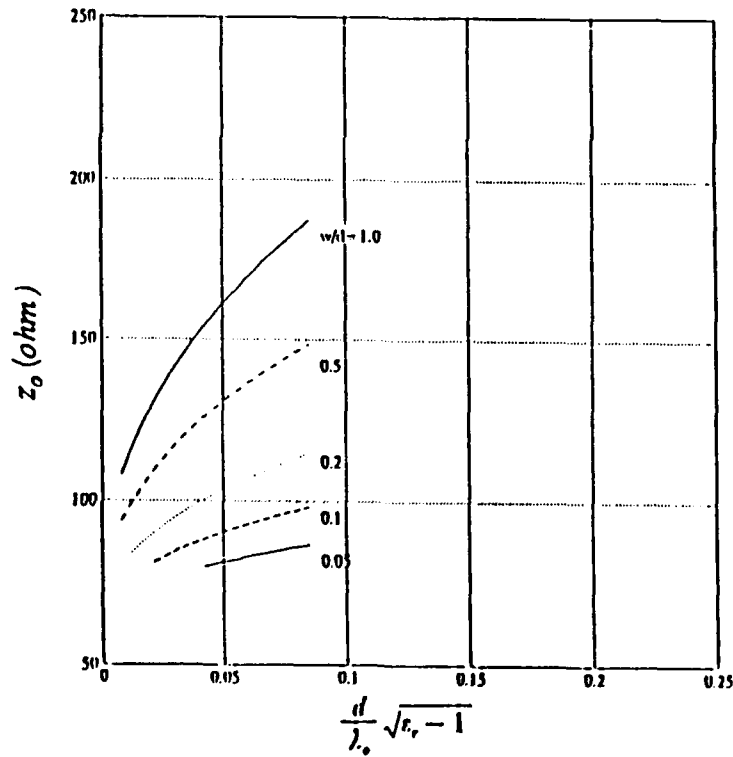
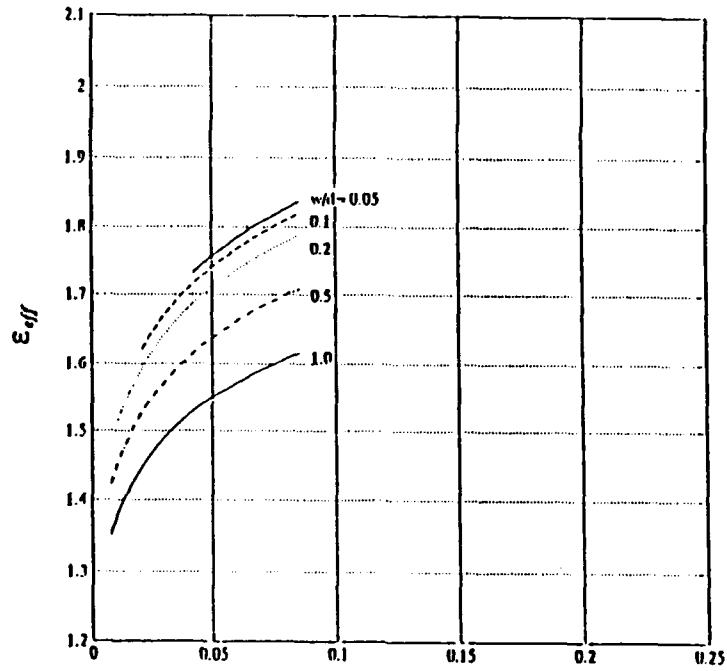


Figure 4.  $\epsilon_{eff}$  and  $Z_0$  versus  $\frac{d}{\lambda_0} \sqrt{\epsilon_r} - 1$ , for  $\epsilon_r = 3.0$ .

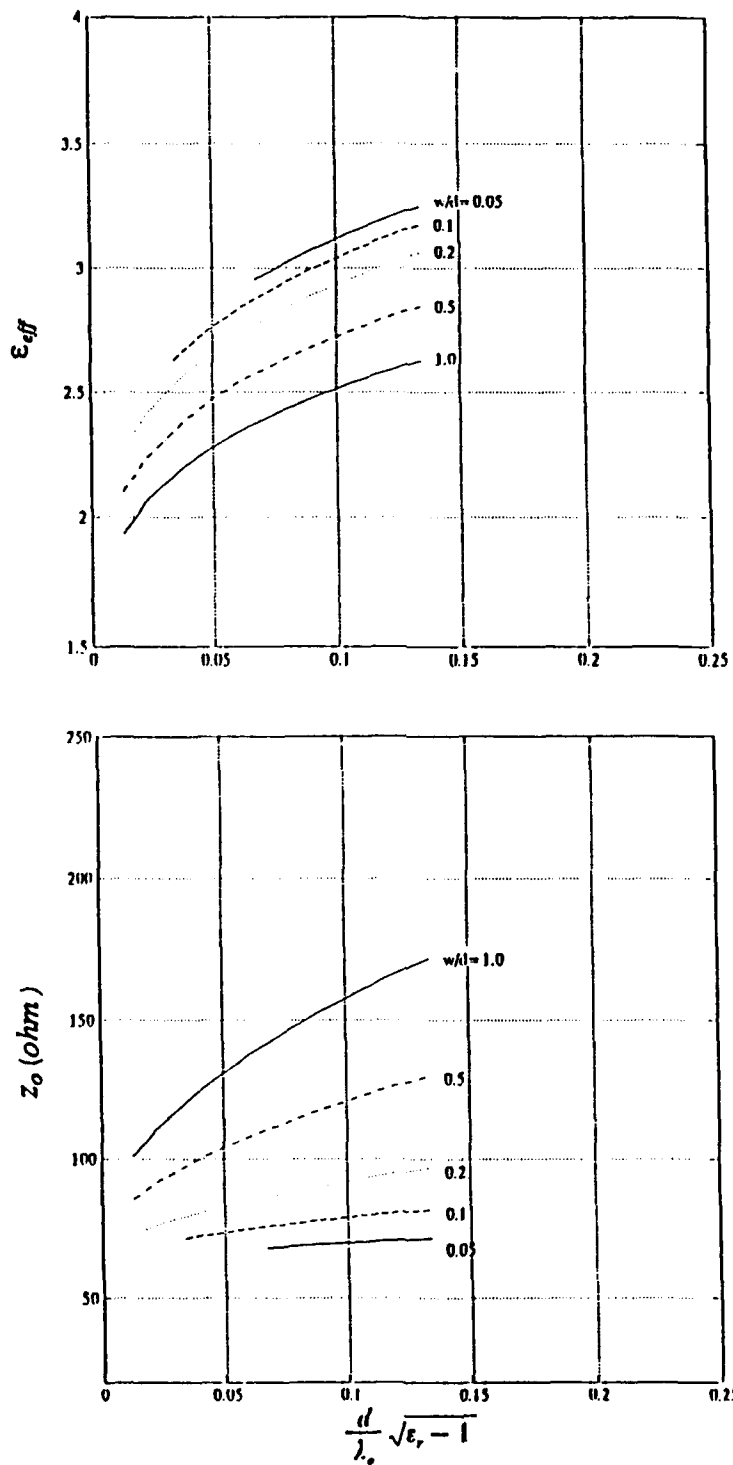


Figure 5.  $\epsilon_{eff}$  and  $Z_0$  versus  $\frac{d}{\lambda_0} \sqrt{\epsilon_r - 1}$ , for  $\epsilon_r = 6.0$ .



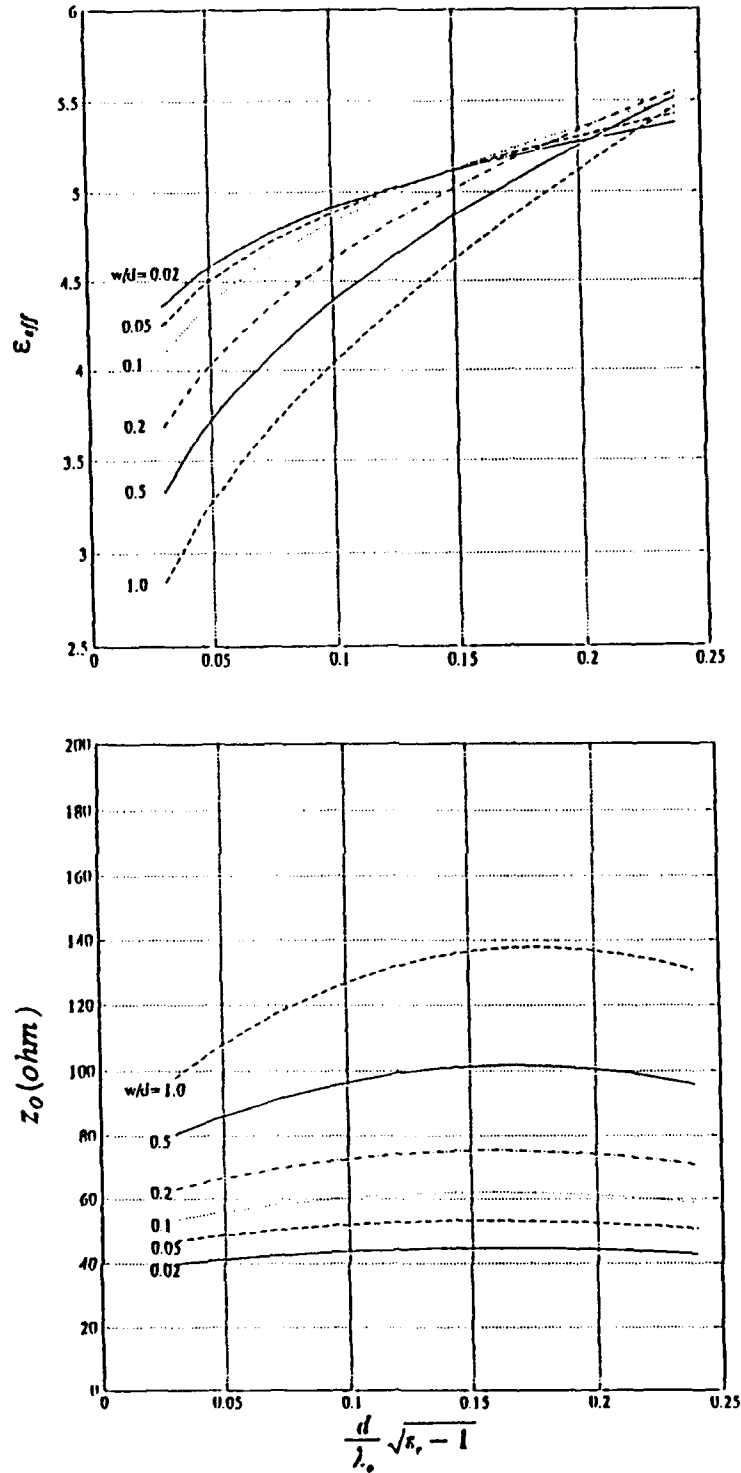


Figure 6.  $\epsilon_{eff}$  and  $Z_0$  versus  $\frac{d}{\lambda_0} \sqrt{\epsilon_r - 1}$ , for  $\epsilon_r = 10.0$ .

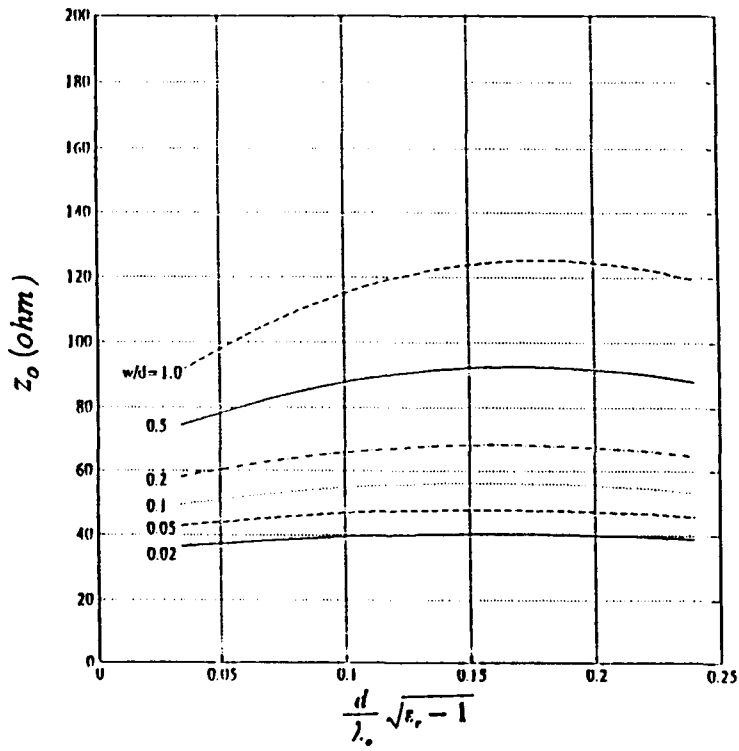
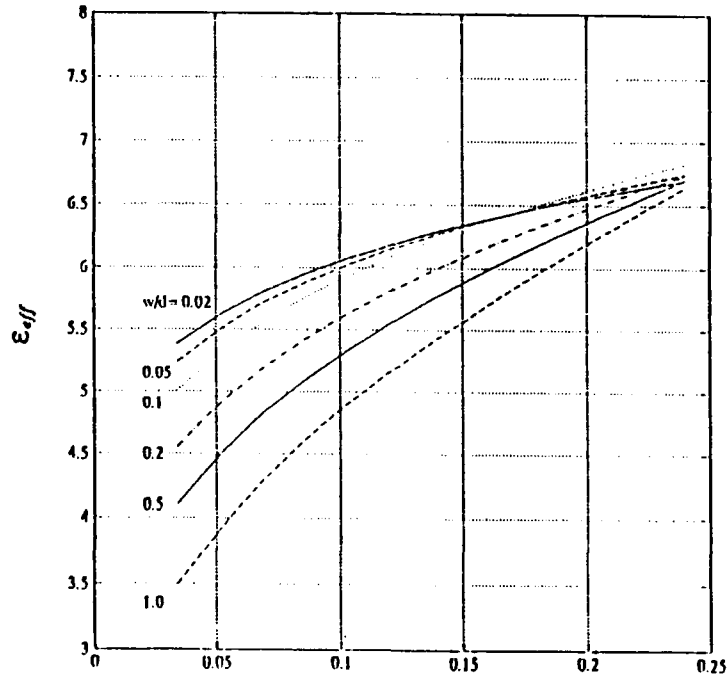


Figure 7.  $\epsilon_{eff}$  and  $Z_0$  versus  $\frac{d}{\lambda_0} \sqrt{\epsilon_r} - 1$ , for  $\epsilon_r = 12.8$ .

### III. BILATERAL SLOTLINE

Although single-sided slotlines have been in use for quite some time as transmission lines and circuits [Ref. 4], slotlines are increasingly being utilized these days in the development of wideband microwave and millimeter-wave antennas [Ref. 1]. A microstrip-to-slotline or a coaxial-to-slotline transition is often needed to couple energy from the feed line to the radiating slotline antenna. The resulting structure has the disadvantage of having a radiating feed. In order to reduce radiation loss from the feed, the slotline antenna can be designed using a double-sided board and fed by means of a non-radiating feed such as a stripline. A double-sided slotline has two identical slots on the opposite sides of a dielectric substrate and arranged one on top of the other without any lateral displacement. We call such a transmission line the *bilateral slotline* [Ref. 6].

Figure 2 (b) shows the geometry of the bilateral slotline. It consists of symmetric slots of width  $w$  etched on opposite sides of a dielectric substrate of thickness  $2d$  and having a relative permittivity  $\epsilon_r$ . The structure has a plane of symmetry shown in Fig. 2 (b). Because of the symmetry, two modes can propagate on the structure (an odd mode and an even mode). The odd mode is the one in which the tangential electric field in the upper slot is equal in magnitude but opposite in sign to the tangential electric field in the lower slot. The even mode is the one in which the slot electric field is identical on both the upper and the lower slots. Such a mode is supported by a perfect magnetic conductor placed in the plane of symmetry. It is the even mode that will be the topic of discussion

of this chapter. In this chapter we provide the design data for the bilateral slotline.

An important distinction exists between the electric conductor-backed slotline (odd mode in a bilateral slotline) and the magnetic conductor-backed slotline. In an electric conductor-backed slotline, power could leak away from the slot in the lateral direction in the form of a parallel plate waveguide mode. Far away from the slot, the structure resembles a conventional dielectric-filled parallel plate waveguide formed by placing electric conductors on both sides of the substrate. This waveguide supports a TEM mode for which there is no cutoff frequency. The leaky TEM mode must be considered as an integral part of the slotline mode during the analysis. However, in the magnetic conductor-backed slotline, the dielectric-filled parallel plate waveguide has an electric conductor on one side (plane containing the slot), but a magnetic conductor on the other side of the substrate. The dominant mode in this structure has a cutoff frequency and will not be excited for  $\frac{d}{\lambda_0} \sqrt{\epsilon_r} < 0.25$ , where  $\lambda_0$  is the free space wavelength. For the dominant mode, the electric field in the upper and lower slots is equal in magnitude and orientation. Like the slotline, it is a non-TEM transmission line. However, it offers two advantages compared to the single-sided slotline. For a given voltage across the slot, both the slots carry power, and, thus, one may expect its power-voltage characteristic impedance to be approximately one-half of that of the corresponding single-sided slotline. Further, the slotline can now be fed by a non-radiating feed such as a stripline. The corresponding antennas in Fig. 1 and 8 would have identical tapered slots on both sides of the dielectric substrate. Theoretical design curves for the bilateral slotline have been obtained

in [Ref. 6] and are shown in Figs. 9 through 13. A computer program has been developed [Ref. 6] to calculate the slot wavelength and the characteristic impedance for a given set of substrate parameters and frequency.

In this chapter we present design data for the evenmode characteristics. Only the dominant mode is considered. As in the case of single-sided slotline, curves for effective dielectric constant  $\epsilon_{eff}$  (the inverse of square of the normalized slot wavelength  $\lambda_s/\lambda_0$ ) and the characteristic impedance  $Z_0$  (based on the power-voltage definition:  $Z_0 = |V|^2/2P$ , where  $V$  is the r m s transverse voltage across the slot, and  $P$  is the average power carried by each slot) are provided for  $\epsilon_r = 2.22, 3.0, 6.0, 10.0, 12.8$  and for  $0.01 \leq \frac{d}{\lambda_0} \sqrt{\epsilon_r - 1} \leq 0.25$ . Using these curves (Figs. 9 - 13) the slot width required to provide a 75 ohm characteristic impedance can be found.

For a fixed substrate thickness of  $2d = 50$  mils, we obtain from Figs. 9 through 13 that  $w = 8.125$  mils, 9.85 mils, 17 mils, 25.25 mils, and 30.65 mils for  $\epsilon_r = 2.22, 3.0, 6.0, 10.0,$  and 12.8 respectively.

When compared to the slot widths required for a single-sided slotline, we see that the bilateral slotline facilitates the use of wider slots, at least as much as five times that needed for single-sided slotline. Clearly, the bilateral slotline offers an immediate solution to the problem of having to otherwise etch very narrow slots on low dielectric constant substrates.

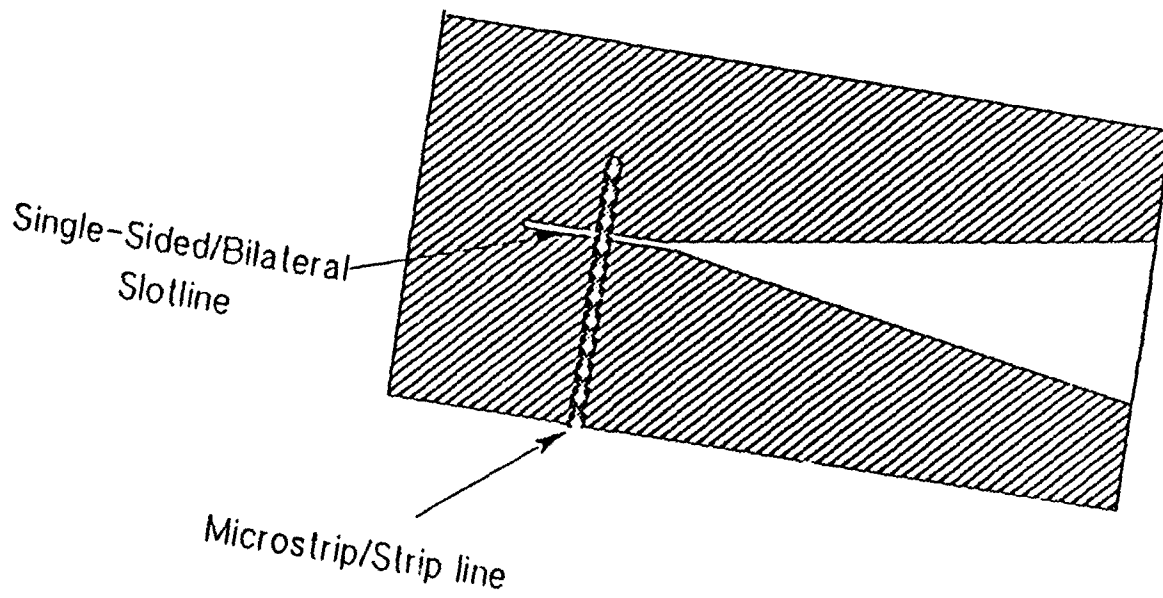


Figure 8. Microstrip-Slotline Transition.

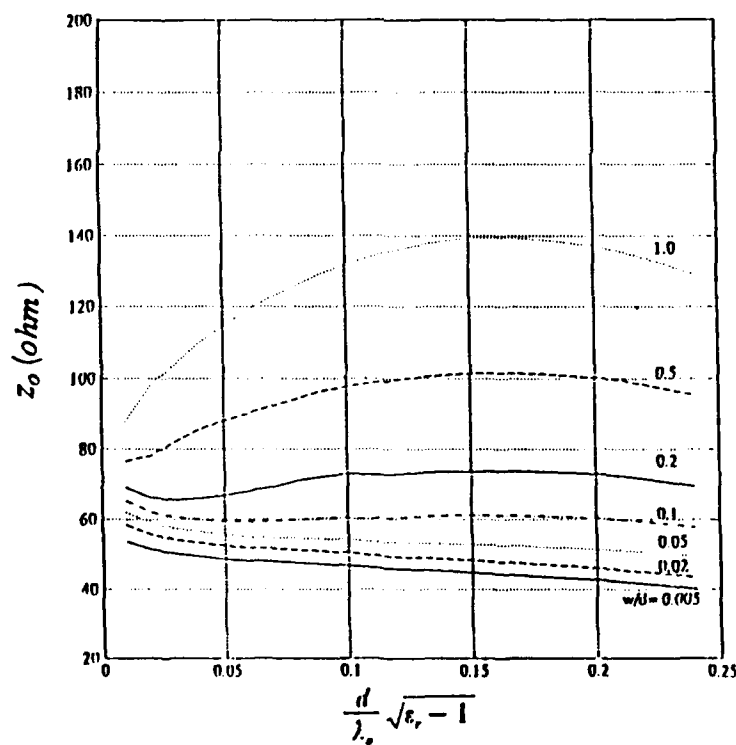
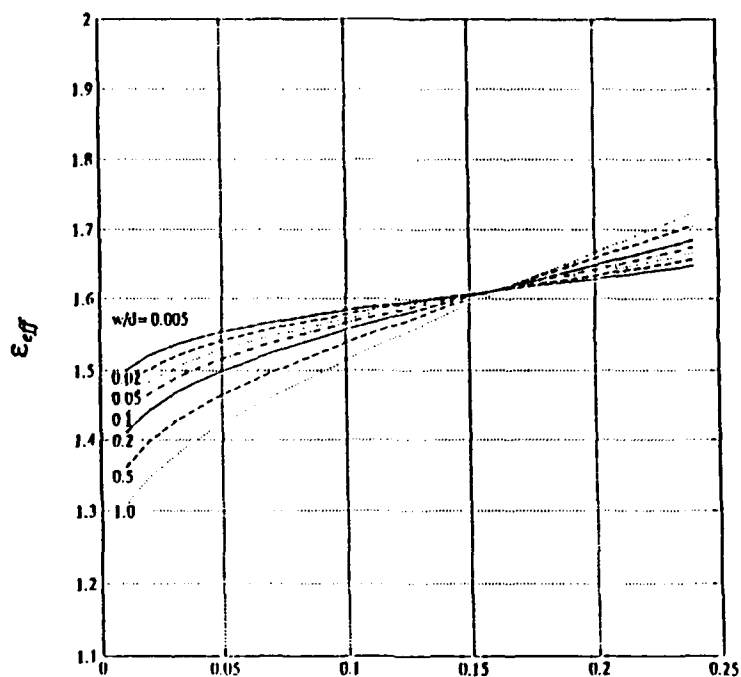


Figure 9.  $\epsilon_{eff}$  and  $Z_0$  versus  $\frac{d}{\lambda_0} \sqrt{\epsilon_r} - 1$ , for  $\epsilon_r = 2.22$ .

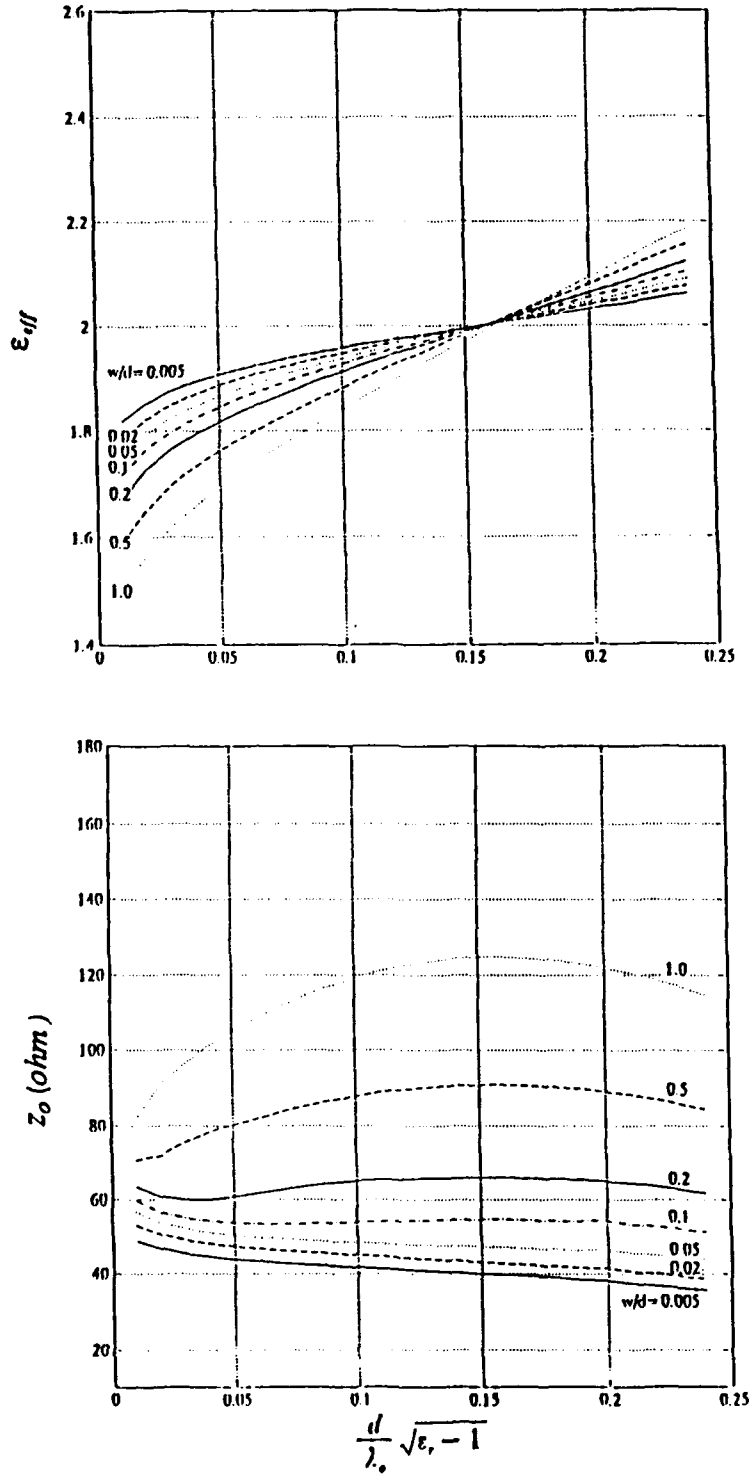


Figure 10.  $\epsilon_{eff}$  and  $Z_0$  versus  $\frac{d}{\lambda_0} \sqrt{\epsilon_r - 1}$ , for  $\epsilon_r = 3.0$ .



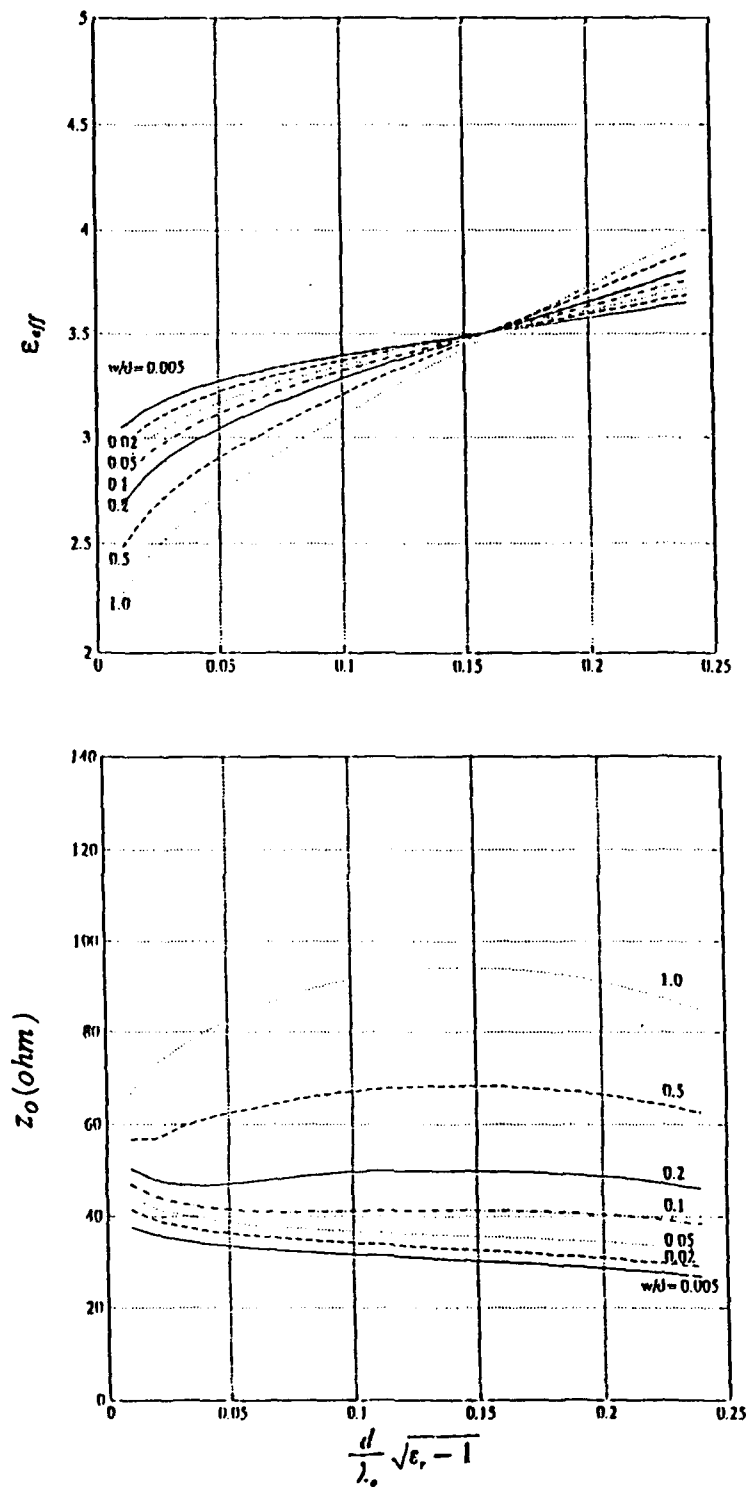


Figure 11.  $\epsilon_{eff}$  and  $Z_0$  versus  $\frac{d}{\lambda_0} \sqrt{\epsilon_r - 1}$ , for  $\epsilon_r = 6.0$ .

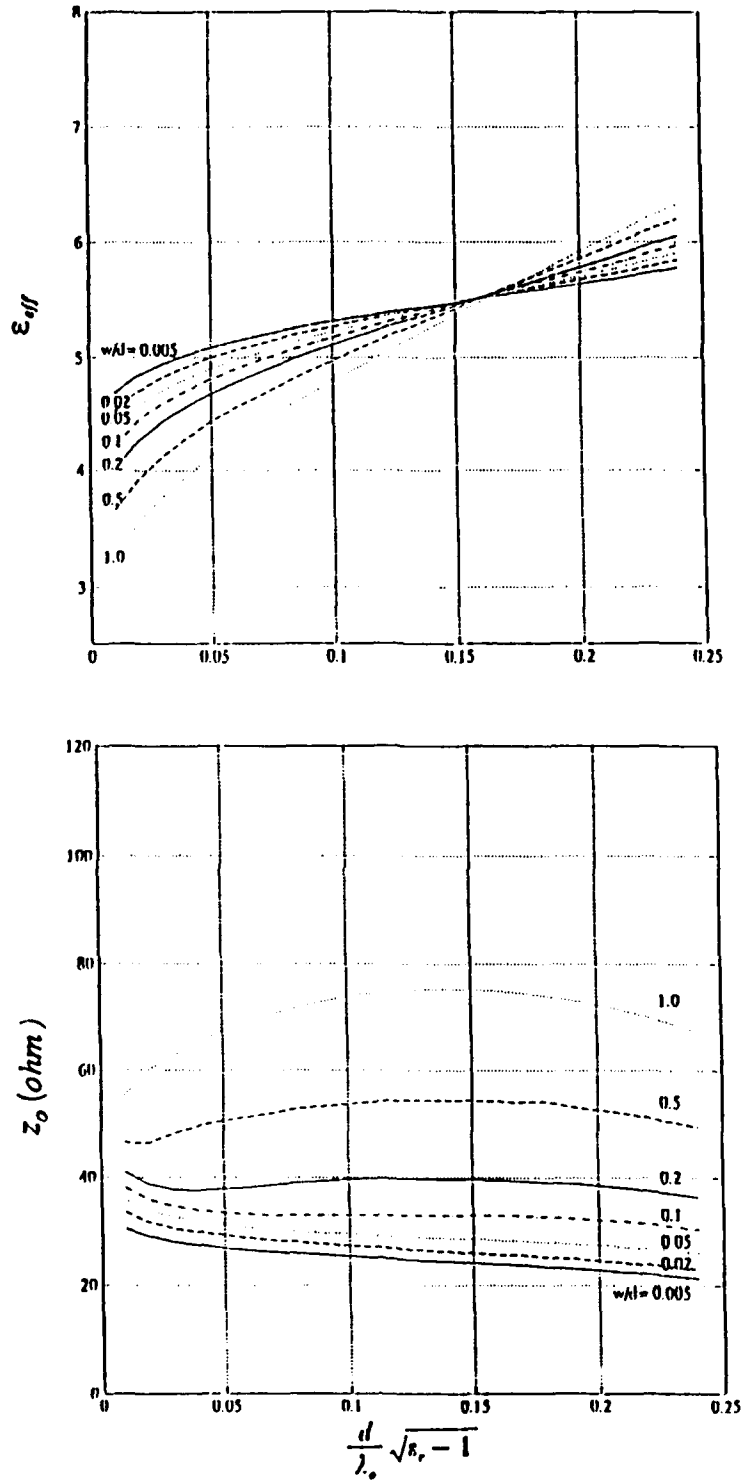


Figure 12.  $\epsilon_{eff}$  and  $Z_0$  versus  $\frac{d}{\lambda_0} \sqrt{\epsilon_r - 1}$ , for  $\epsilon_r = 10.0$ .

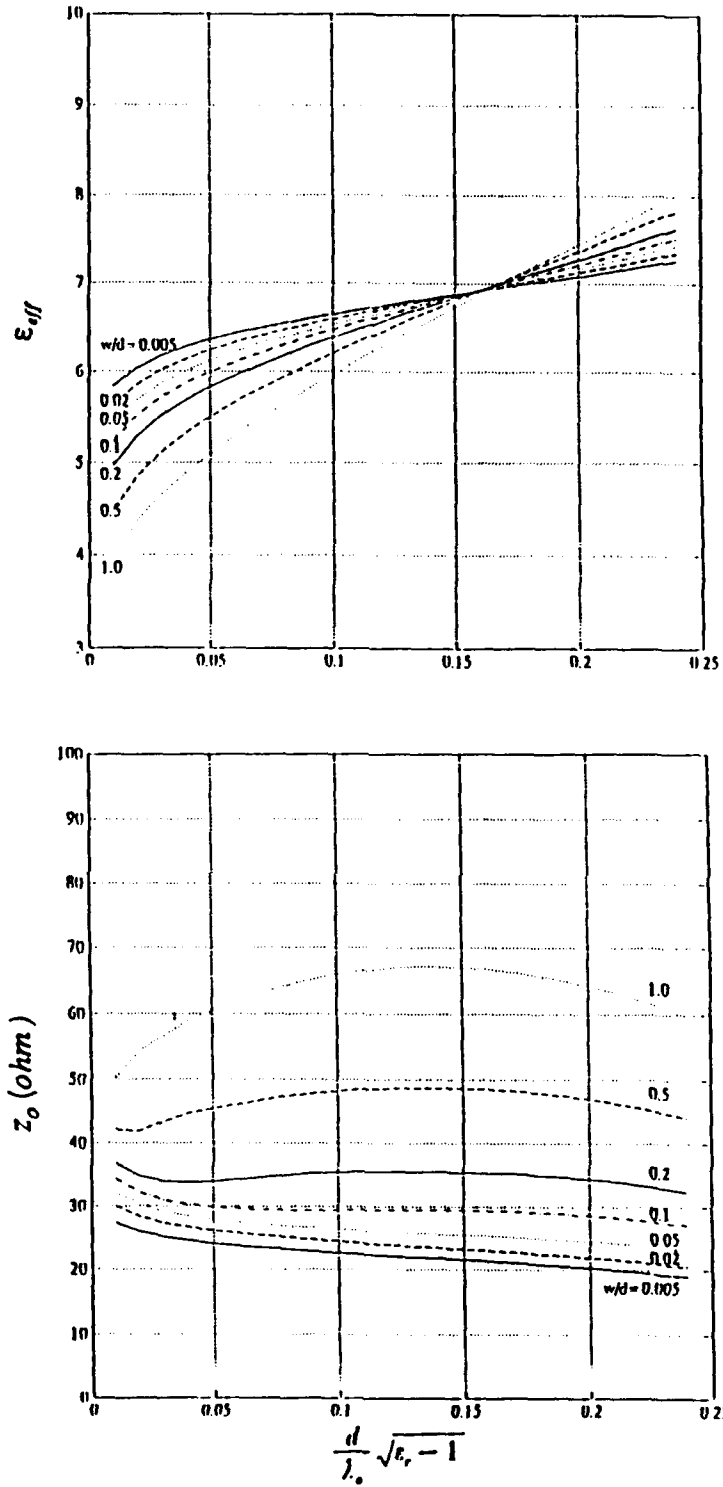


Figure 13.  $\epsilon_{eff}$  and  $Z_0$  versus  $\frac{d}{\lambda_0} \sqrt{\epsilon_r - 1}$ , for  $\epsilon_r = 12.8$ .

#### IV. ASYMMETRIC SLOTLINE

As mentioned in earlier chapters, a microstrip-to-slotline or a coaxial-to-slotline transition is often needed to couple energy from the input transmission line to the slotline feeding the tapered slot antenna of Fig. 1. With single-sided slotline, one is faced with the difficulty of fabricating very narrow slots for the feeding slotline in order to obtain a good impedance match with the input line. To overcome this and other problems associated with the single-sided slotline, *Gvozdev* [Ref. 10] suggested the use of an asymmetric slotline, in which the current-carrying conductors are placed on opposite sides of the dielectric substrate. This structure was effectively used by *Gazit* [Ref. 11] in the design of wideband feeds for the tapered slot antenna. In the present investigation we are concerned with the propagation of the fundamental mode on the asymmetric slotline. The structure has been analyzed using the Wiener-Hopf technique [Ref. 7] and theoretical results presented for the propagation constant and the characteristic impedance of the dominant mode. In this chapter we provide the design data for the asymmetric slotline.

Figure 2 (c) shows the cross-section of the asymmetric slotline. It consists of two semi-infinite conductors placed on opposite sides of a dielectric substrate of thickness  $t = 2d$  and having a relative permittivity  $\epsilon_r$ . Due to the inherent dielectric inhomogeneity of the structure, the guided wave will be non-TEM in nature and will suffer dispersion. Placement of conductors on the opposite sides of the substrate allows one to bring the two edges arbitrarily close to each other

in the lateral direction. In this configuration, etching narrow slots poses no fabrication difficulty as they lie on the opposite sides of the substrate. One may then have a negative width slot (obtained by overlapping the two conductors) or a positive width slot (obtained by non-overlapping conductors) resulting in a wide range of impedances values. After matching to a low impedance transmission line such as a microstrip line, the slot may be flared to obtain the desired radiation characteristics. Figure 14 shows a typical transition between a microstrip line and the asymmetric slotline. Because the electric field lines extend from one interface of the dielectric substrate to the other, the dominant mode in an asymmetric slotline behaves more like the quasi-TEM mode in a microstrip line. Theoretical transmission line characteristics for the case of overlapping conductors have been presented in [Ref.8]. A computer program was developed to get the effective dielectric constant  $\epsilon_{eff}$  (the inverse of square of the normalized slot wavelength  $\lambda_s/\lambda_o$ ) and the characteristic impedance  $Z_o$ . Figures 15 through 19 show the characteristics for  $\epsilon_r = 2.22, 3.0, 6.0, 10.0,$  and  $12.8$  for  $0.01 \leq \frac{d}{\lambda_o} \sqrt{\epsilon_r - 1} \leq 0.25$ . The characteristic impedance  $Z_o$  for the mode has been obtained as the ratio of the transverse voltage between the two conductors at the overlap center to the longitudinal current flowing on one of the conductors ( $Z_o = V/I$ , where  $V$  is the r m s transverse voltage across the substrate, and  $I$  is the r m s current carried by each conductor).

In the microstrip-line-to-asymmetric-slotline transition, one should be able to match the 50 ohm microstrip line to a 50 ohm asymmetric slotline rather than to 75 ohms used in the two previous cases.

To obtain a 50 ohm characteristic impedance with  $t = 50$  mils, we require  $s = 100$  mils, 81 mils, 44.4 mils, 21.25 mils, and 10.5 mils with  $\epsilon_r = 2.22, 3.0, 6.0, 10.0,$  and  $12.8,$  respectively. When compared to the slot widths required for a single-sided slotline, we see that the asymmetric slotline facilitates the use of wider slots, at least as much as fifty times that needed for single-sided slotline. Further, etching narrow slots poses no problem as conductors are arranged on opposite sides of the substrate.

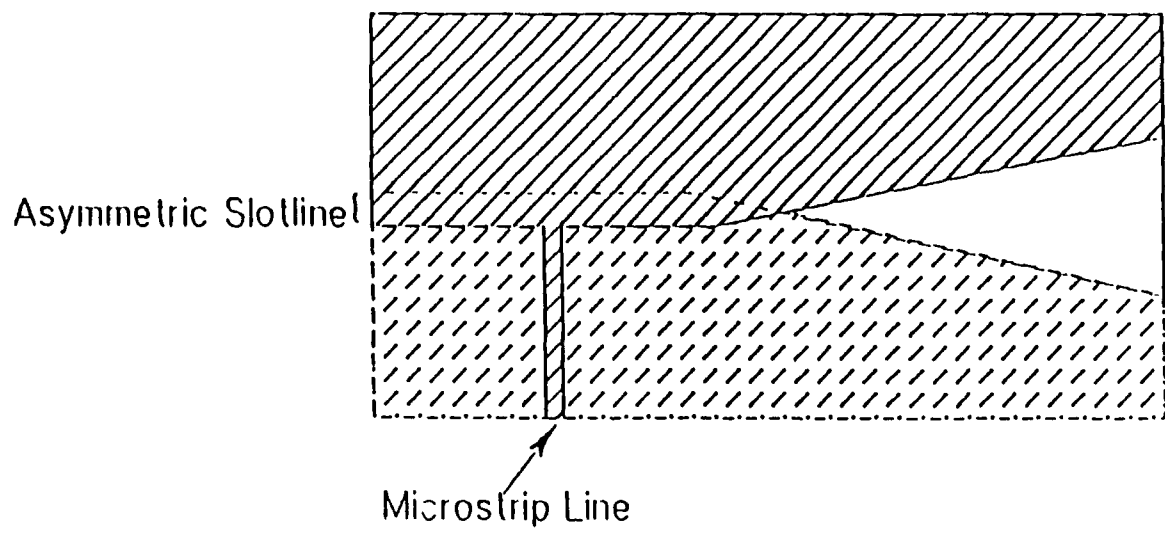


Figure 14. Microstrip line-Asymmetric Slotline Transition.

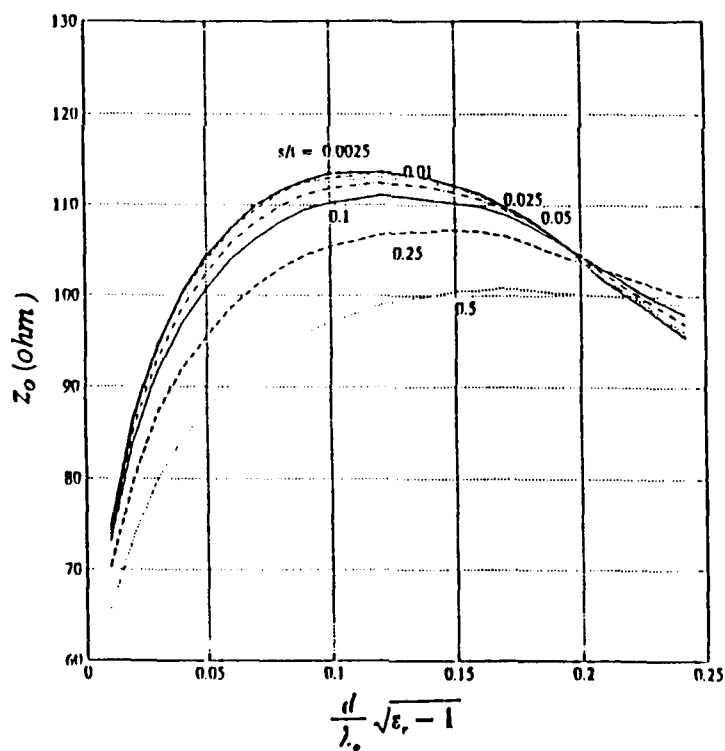
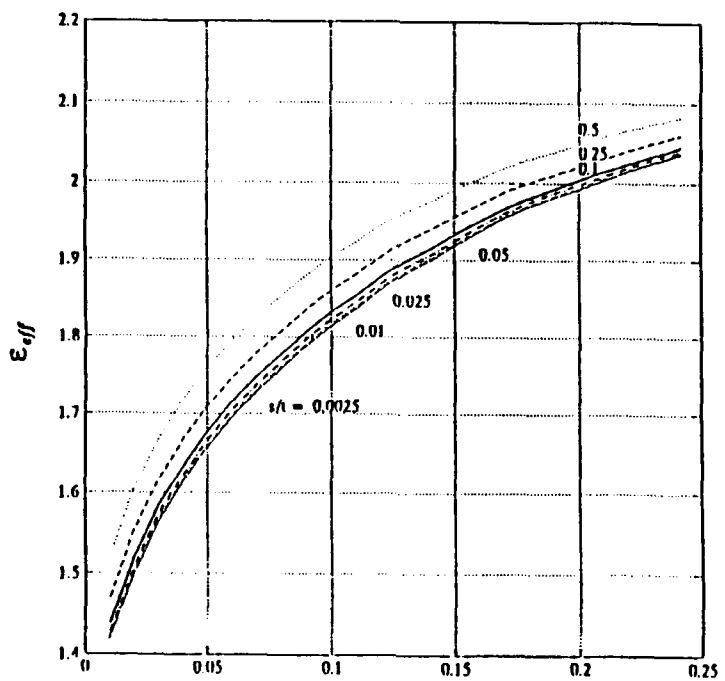


Figure 15.  $\epsilon_{eff}$  and  $Z_0$  versus  $\frac{d}{\lambda_0} \sqrt{\epsilon_r} - 1$ , for  $\epsilon_r = 2.22$ .



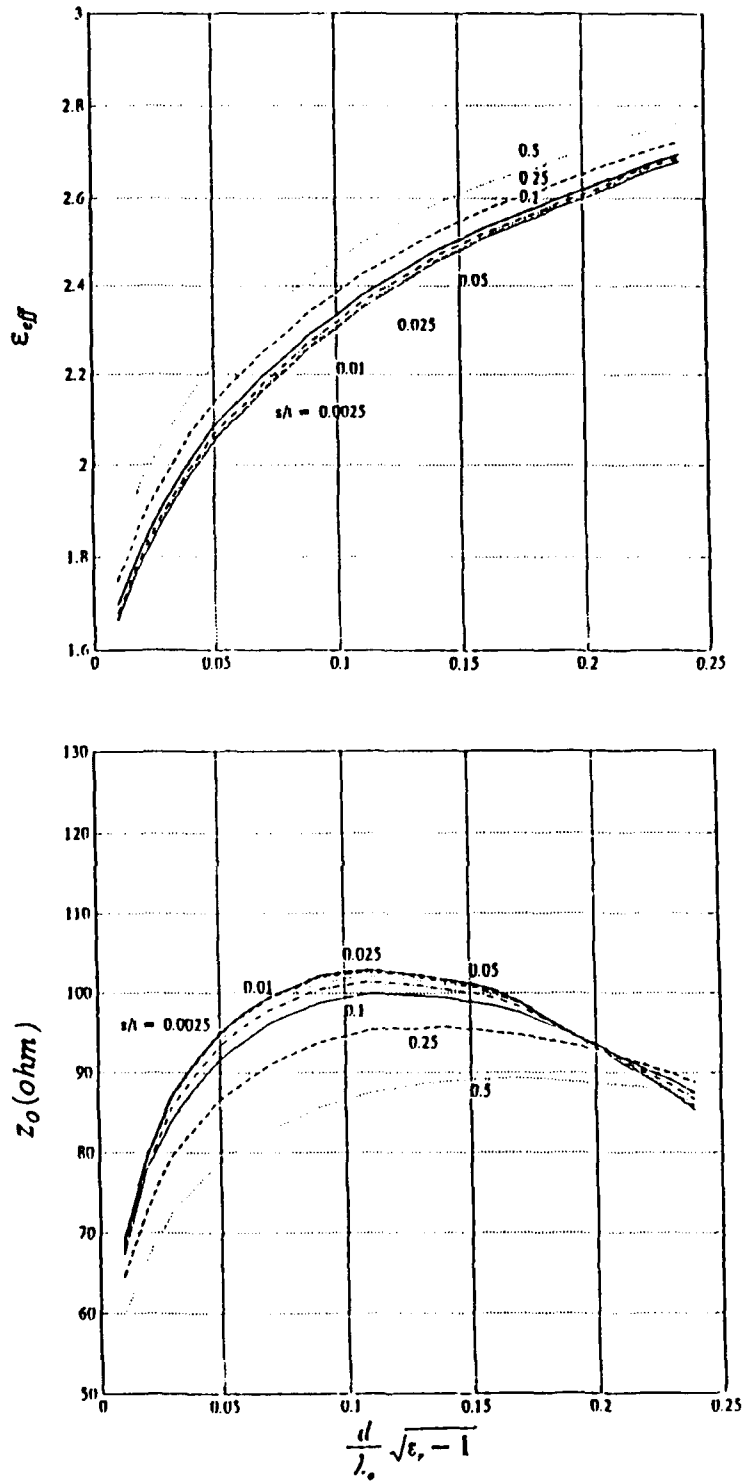


Figure 16.  $\epsilon_{eff}$  and  $Z_0$  versus  $\frac{d}{\lambda_0} \sqrt{\epsilon_r - 1}$ , for  $\epsilon_r = 3.0$ .

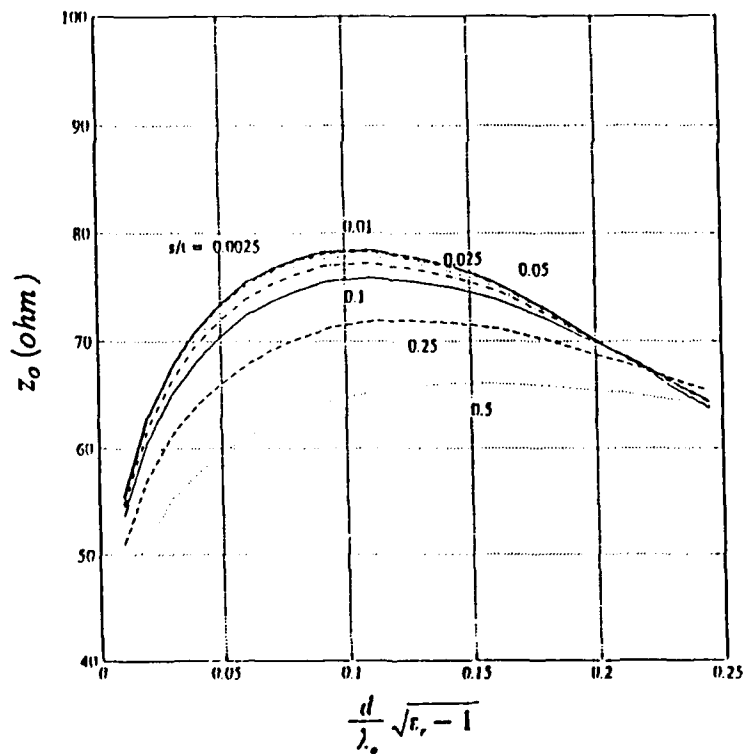
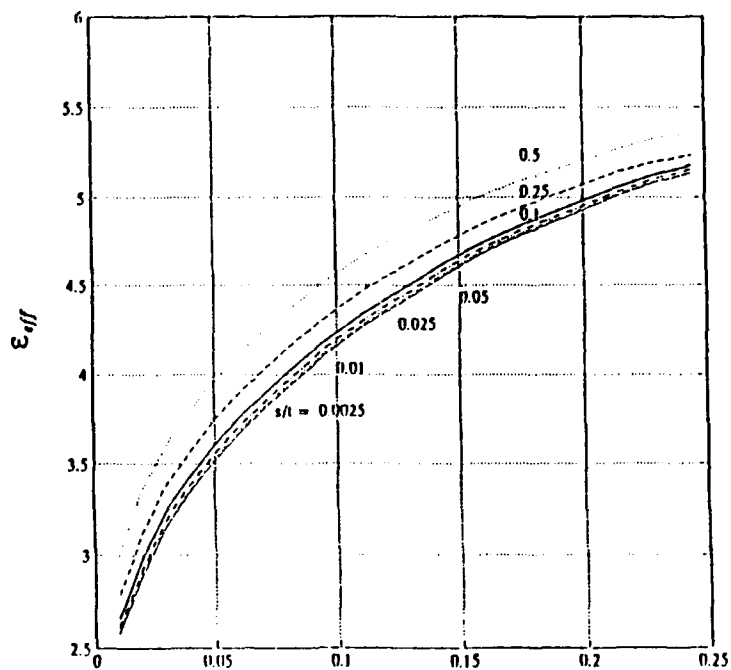


Figure 17.  $\epsilon_{eff}$  and  $Z_0$  versus  $\frac{d}{\lambda_0} \sqrt{\epsilon_r - 1}$ , for  $\epsilon_r = 6.0$ .

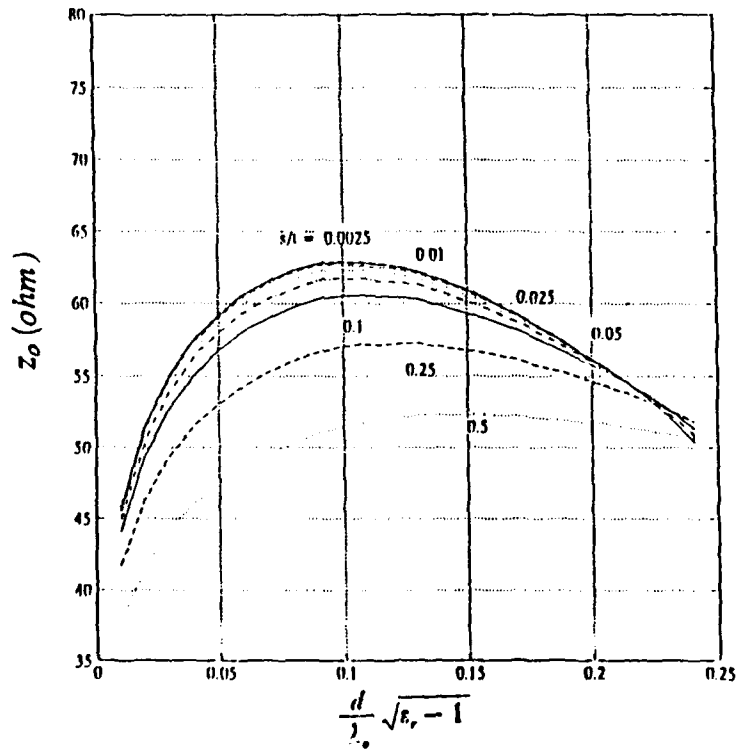
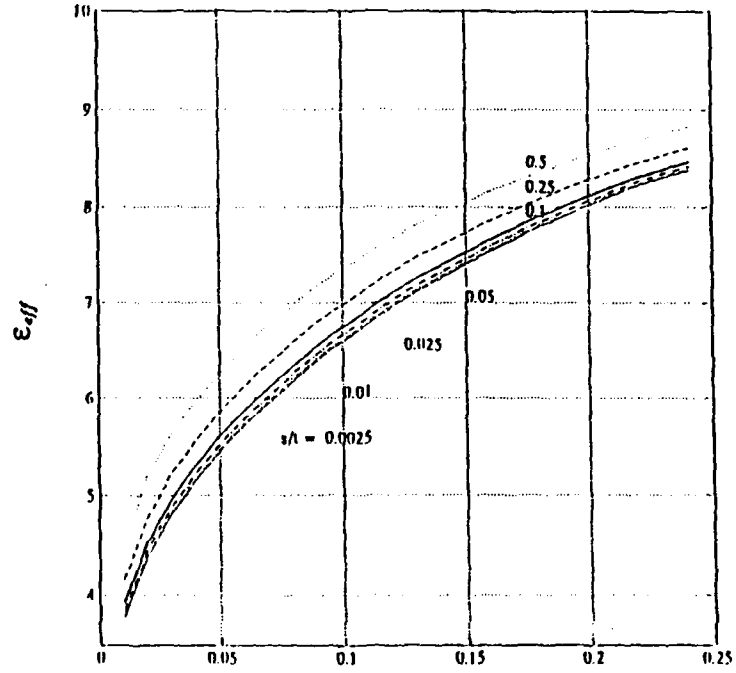


Figure 18.  $\epsilon_{eff}$  and  $Z_0$  versus  $\frac{d}{\lambda_0} \sqrt{\epsilon_r - 1}$ , for  $\epsilon_r = 10.0$ .

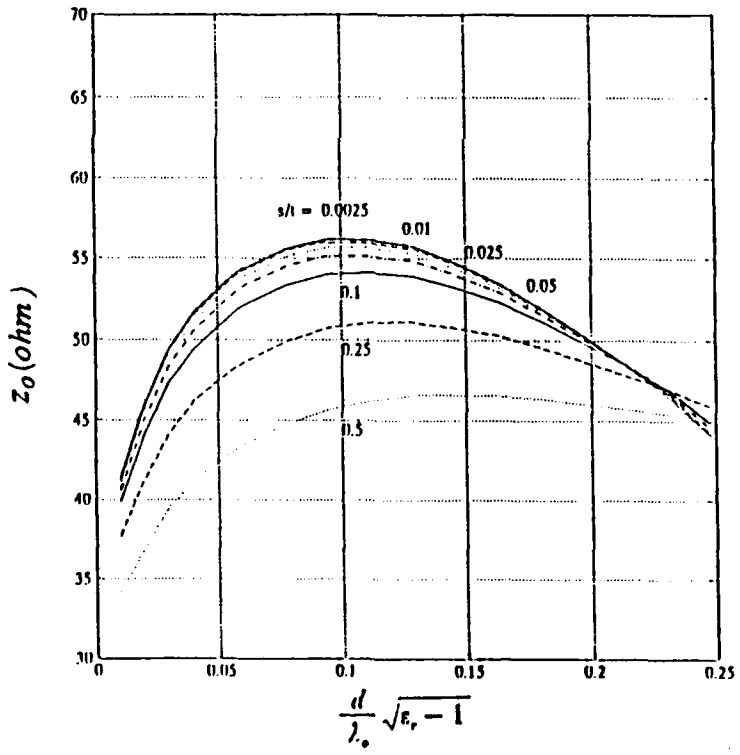
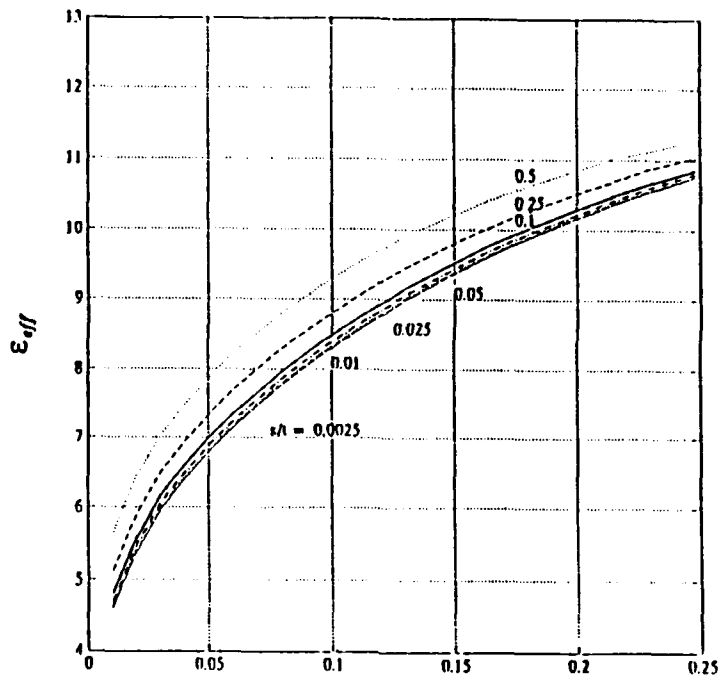


Figure 19.  $\epsilon_{eff}$  and  $Z_0$  versus  $\frac{d}{\lambda_0} \sqrt{\epsilon_r - 1}$ , for  $\epsilon_r = 12.8$ .

## V. CONCLUSION

Design curves for slotline characteristics have been provided for a single-sided slotline, bilateral slotline and the asymmetric slotline. It has been shown that single-sided slotline suffers the disadvantage of producing narrow slots on low- $\epsilon_r$  substrates to realize nominal impedance values. This is primarily because the single-sided slotline is a high impedance line. A double-sided slotline carries approximately twice as much power as a single-sided slotline for the same voltage across the slot. Consequently, for the same substrate and slot parameters, its characteristic impedance is approximately one half of the latter. Alternately, it facilitates the use of wider slots on low- $\epsilon_r$  substrates than does the single-sided slotline. Further, the stripline-to-bilateral-slotline transition is non-radiative. A second way to overcome the problem associated with a single-sided slotline is to place conductors on opposite sides of the substrate. Overlapping conductors are then possible resulting in low impedance values. The slot parameters needed to achieve a given low impedance, such as 50 ohms, are better realizable in an asymmetric slotline. The bilateral and the asymmetric slotlines should serve as possible alternatives to a regular single-sided slotline in the design of printed circuits. Design curves for all these slotlines have been provided for  $2.22 \leq \epsilon_r \leq 12.8$  and for  $0.01 \leq \frac{d}{\lambda_0} \sqrt{\epsilon_r - 1} \leq 0.25$ . These curves should serve as useful design guidelines in the design of circuits and antennas making use of these lines.

## APPENDIX A. THE PROGRAM OF THE SINGLE-SIDED SLOTLINE

C THIS PROGRAM SHOWS THE VALUES OF Eeff & Z0 OF THE SINGLE-SIDED SLOTLINE

```

REAL Er, WBYD, DBYLO, WBYLO, EFTHCK, Eeff1, Z01, Eeff2, Z02, Eeff3, Z03
REAL Eeff4, Z04, Eeff5, Z05, Eeff6, Z06, PI, A, B, C, D, E, F, G, H, K, L, M, Q
REAL LBL1, LBL2, LBL3, LBL4, LBL5, LBL6
CHARACTER*10 OUTFILE
PI = 4.0*ATAN(1.0)
OPEN ( 10 , FILE = 'INDATA0' )
PRINT*, 'NAME OF OUTPUT FILE? '
READ(5,*) OUTFILE
OPEN ( 20 , FILE = OUTFILE )
DO 100 I = 1,744
READ (10,*) Er , WBYD , DBYLO
WBYLO = WBYD*DBYLO
EFTHCK = DBYLO*(Er - 1.0)**0.5
IF(EFTHCK.GT.0.0 .AND. EFTHCK.LT.0.25) THEN
  IF(Er.GE.2.22 .AND. Er.LE.3.8) THEN
    IF(WBYLO.GE.0.0015 .AND. WBYLO.LT.0.075) THEN
      LBL1 = 1.045 - 0.365*ALOG(Er) + (6.3*WBYD*Er**0.945)/
+      (238.64 +100*WBYD) - (0.148-(8.81*(Er+0.95))/(100*Er))
+      *ALOG(DBYLO)
      Eeff1 = 1/LBL1**2
      A = ((Er-2.22)*PI)/2.36
      B = 10*Er
      Q = 100*DBYLO
      Z01 = 60.0 + 3.69*SIN(A) + 133.5*ALOG(B)*WBYLO**0.5
+      + 2.81*(1 - 0.011*Er*(4.48+ALOG(Er)))*WBYD*ALOG(Q)
+      + 131.1*(1.028-ALOG(Er))*DBYLO**0.5 + 12.48*
+      (1+0.18*ALOG(Er))*WBYD/(Er-2.06 + 0.85*WBYD**2)**0.5
C      WRITE(20,11)
C      FORMAT(2X,'Er',8X,'W/D',6X,'D/L0',5X,'W/L0',6X,'EFTHCK',
C      + 2X,'Eeff1',7X,'Z01',6X,'LBL1')
C      WRITE(20,12) Er,WBYD,DBYLO,WBYLO,EFTHCK,Eeff1,Z01,LBL1
12      FORMAT(' ',F5.2,4X,F5.3,4X,F5.3,4X,F6.4,4X,F5.3,4X,F6.3,4X,
+      F8.3,2X,F6.3)
C      WRITE(20,13)
C      FORMAT(1X,'          ')
    ELSE
      IF(WBYLO.GE.0.075 .AND. WBYLO.LE.1.0) THEN
        LBL2 = 1.194 - 0.24*ALOG(Er) -
+        (0.621*Er**0.835*WBYLO**0.48)/
+        (1.344+WBYD) - 0.0617*(1.91-(Er+2)/Er)
+        *ALOG(DBYLO)

```

```

Eeff2 = 1/LBL2**2
Z02 = 133+10.34*(Er-1.8)**2 + 2.87
+      *(2.96+(Er-1.582)**2)*((WBYD+
+      2.32*Er-0.56)*((32.5-6.67*Er)
+      *(100*DBYLO)**2-1))**0.5-
+      (684.45*DBYLO)*(Er+1.35)**2+13.23
+      *((Er-1.722)*WBYLO)**2
C      WRITE(20,21)
C      FORMAT(2X,'Er',8X,'W/D',6X,'D/LO',5X,'W/LO',6X,'EFTHCK',
C      +      2X,'Eeff2',7X,'Z02',6X,'LBL2')
C      WRITE(20,22) Er,WBYD,DBYLO,WBYLO,EFTHCK,Eeff2,Z02,LBL2
22     FORMAT(' ',F5.2,4X,F5.3,4X,F5.3,4X,F6.4,4X,F5.3,4X,F6.3,
+      4X,F8.3,2X,F6.3)
C      WRITE(20,23)
C      FORMAT(1X,'          ')
      ENDIF
    ENDIF
  ELSE
    IF(Er.GE.3.8 .AND. Er.LE.9.8) THEN
      IF(WBYLO.GE.0.0015 .AND. WBYLO.LT.0.075) THEN

        LBL3 = 0.9217-0.277*ALOG(Er)+0.0322*WBYD
+          *(Er/(WBYD+0.435))**0.5 -0.01*ALOG(DBYLO)
+          *(4.6-3.65/(Er**2*WBYLO**0.5*(9.06-100*WBYLO)))
        Eeff3 = 1/LBL3**2
        C = 100*DBYLO
        Z03 = 73.6-2.15*Er+(638.9-31.37*Er)
+          *WBYLO**0.6+(36.23*(Er**2+41)
+          **0.5-225)*WBYD/(WBYD+0.876*Er-2)
+          +0.51*(Er+2.12)*WBYD
+          *ALOG(C)-0.753*Er*DBYLO/WBYLO**0.5
C      WRITE(20,31)
C      FORMAT(2X,'Er',8X,'W/D',6X,'D/LO',5X,'W/LO',6X,'EFTHCK',
C      +      2X,'Eeff3',7X,'Z03',6X,'LBL3')
C      WRITE(20,32) Er,WBYD,DBYLO,WBYLO,EFTHCK,Eeff3,Z03,LBL3
32     FORMAT(' ',F5.2,4X,F5.3,4X,F5.3,4X,F6.4,4X,F5.3,4X,F6.3,
+      4X,F8.3,2X,F6.3)
C      WRITE(20,33)
C      FORMAT(1X,'          ')
      ELSE
        IF(WBYLO.GE.0.075 .AND. WBYLO.LE.1.0) THEN
          D = WBYD-2.012*(1-0.146*Er)
          E = 14.7-Er
          LBL4 = 1.05-0.04*Er+1.411*0.01*(Er-1.421)
+          *ALOG(D)+0.111*(1-0.366*
+          Er)*WBYLO**0.5+0.139*(1+0.52*Er
+          *ALOG(E))*DBYLO*ALOG(DBYLO)
          Eeff4 = 1/LBL4**2
          F = 2*Er
          G = 1.11+0.132*(Er-27.7)/(100*DBYLO+5)
        ENDIF
      ENDIF
    ENDIF
  ENDIF

```

```

H = 100*DBYLO+((100*DBYLO)**2+1)**0.5
Z04 = 120.75-3.74*Er+50*(ATAN(F)-0.8)
+      *WBVD**G*ALOG(H)+14.21*
+      (1-0.458*Er)*(100*DBYLO+5.1
+      *ALOG(Er)-13.1)*(WBVD+0.33)**2
C      WRITE(20,41)
C      FORMAT(2X,'Er',8X,'W/D',6X,'D/LO',5X,'W/LO',6X,'EFTHCK',
C      +      2X,'Eeff4',7X,'Z04',6X,'LBL4')
42     WRITE(20,42) Er,WBVD,DBYLO,WBVD,EFTHCK,Eeff4,Z04,LBL4
+     FORMAT(' ',F5.2,4X,F5.3,4X,F5.3,4X,F6.4,4X,F5.3,4X,F6.3,
C      +      4X,F8.3,2X,F6.3)
C      WRITE(20,43)
C      FORMAT(1X,'          ')
      ENDIF
      ENDIF
      ENDIF
      IF(Er.GE.9.8 .AND. Er.LE.20.0) THEN
      IF(WBVD.GE.0.02 .AND. WBVD.LT.0.2) THEN
      K= DBYLO*100
      L= WBVD*100
      LBL5= 0.923-0.448*ALOG10(Er) +0.2
+      *WBVD-(0.29*WBVD+0.047)*ALOG10(K)
      Eeff5 = 1/LBL5**2
      Z05 = 72.62 - 35.19*ALOG10(Er)
+      + 50*(WBVD-0.02)*
+      (WBVD-0.1)/WBVD+ALOG10(L)
+      *( 44.28- 19.58*ALOG10(Er))
+      -(0.32*ALOG10(Er)-0.11
+      +WBVD*(1.07*ALOG10(Er)+1.44))
+      *(11.4-6.07*ALOG10(Er)-K)**2
C      WRITE(20,51)
C      FORMAT(2X,'Er',8X,'W/D',6X,'D/LO',5X,'W/LO',6X,'EFTHCK',
C      +      2X,'Eeff5',7X,'Z05',6X,'LBL5')
52     WRITE(20,52) Er,WBVD,DBYLO,WBVD,EFTHCK,Eeff5,Z05,LBL5
+     FORMAT(' ',F5.2,4X,F5.3,4X,F5.3,4X,F6.4,4X,F5.3,4X,F6.3,
C      +      4X,F8.3,2X,F6.3)
C      WRITE(20,53)
C      FORMAT(1X,'          ')
      ELSE
      IF(WBVD.GE.0.2 .AND. WBVD.LE.1.0) THEN
      M = 100*DBYLO
      LBL6 = 0.987-0.483*ALOG10(Er) + WBVD*(0.111
+      - 0.0022*Er)- (0.121+0.094*WBVD- 0.0032*Er)
+      *ALOG10(M)
      Eeff6 = 1/LBL6**2
      Z06 = 113.19 - 53.55*ALOG10(Er) + 1.25*(WBVD)
+      *(114.59 - 51.88* ALOG10(Er)) +20*(WBVD- 0.2)
+      *(1-WBVD)- (0.15 +0.23*ALOG10(Er) +WBVD
+      *(-0.79+2.07*ALOG10(Er)))*(10.25- 5*ALOG10(Er)
+      +WBVD*(2.1- 1.42*ALOG10(Er))- M)**2
C      WRITE(20,61)

```



```

C          FORMAT(2X,'Er',8X,'W/D',6X,'D/LO',5X,'W/LO',6X,'EFTHCK',
C      +    2X,'Eeff6',7X,'Z06',6X,'LBL6')
          WRITE(20,62) Er,WBYD,DBYLO,WBYLO,EFTHCK,Eeff6,Z06,LBL6
62          FORMAT(' ',F5.2,4X,F5.3,4X,F5.3,4X,F6.4,4X,F5.3,4X,F6.3,
C      +    4X,F8.3,2X,F6.3)
C          WRITE(20,63)
C          FORMAT(1X,'          ')
          ENDIF
          ENDIF
          ENDIF
          ENDIF
          ENDIF
100        CONTINUE
          END

```

## LIST OF REFERENCES

1. K. S. Yngvesson, T. L. Korzeniowski, Y. S. Kim, E. L. Kollberg, and J. F. Johansson, "The Tapered Slot Antenna-A New Integrated Element for Millimeter Wave Applications," IEEE Trans. Microwave Theory Tech., Vol. MTT-37, No. 2, pp. 365-374, February 1989.
2. Y. H. Choung and C. C. Chen, "44 GHz Slotline Phased Array Antenna," 1989 IEEE AP-S International Symposium Digest, Vol.III, Paper # AP-78-4, pp. 1730-1733, 1989.
3. R. Janaswamy and D. H. Schaubert, "Analysis of the Tapered Slot Antenna," IEEE Trans. Antennas Propagat., Vol AP-35, No. 9, pp. 1058-1065, September 1987.
4. K. C. Gupta, R. Garg, and I. J. Bahl, *Microstrip Lines and Slotlines*, Artech House, Dedham, Massachusetts, 1979.
5. R. Janaswamy and D. H. Schaubert, "Characteristic Impedance of a Wide Slotline on Low-Permittivity Substrates," IEEE Transactions on Microwave Theory and Techniques, Vol. MTT-34, No. 8, pp. 899-902, Aug. 1986.
6. R. Janaswamy, "Even Mode Characteristics of The Bilateral Slotline," to appear in the IEEE Transactions on Microwave Theory and Techniques, Vol. MTT-38, No. 6, June 1990.
7. R. Janaswamy, "Wiener-Hopf Analysis of The Asymmetric Slotline," to appear, Radio Science.
8. R. Janaswamy, "Comparison of Slotlines for Planar Antennas," Proceedings, 1990 MIC Workshop, San Diego, organized by Arlon Microwave Material Division, March 1990.
9. J. B. Knorr, "Slotline Transitions," IEEE Trans. Microwave Theory Tech., Vol. MTT-22, pp. 548-554, May 1974.

10. V. I. Gvozdev, "Use of Unbalanced Slotted Line in SHF Microcircuits," Radio Engr. & Electron Physics, Vol. MTT-27, No. 11, pp. 42-47, 1982.
11. E. Gazit, "Improved Design of the Vivaldi Antenna," IEE Proceedings, 135, Pt. H, No. 2, pp. 89-92, 1988.

## INITIAL DISTRIBUTION LIST

	No. Copies
1. Defense Technical Information Center Cameron Station Alexandria, VA 22304-6145	2
2. Library, Code 0142 Naval Postgraduate School Monterey, CA 93943-5002	2
3. Chairman, Code EC Department of Electrical and Computer Engineering Naval Postgraduate School Monterey, CA 93943-5000	2
4. Curricular Officer Code 32 Naval Postgraduate School Monterey, CA 93943-5000	1
5. Prof. R. Janaswamy, Code EC/Js Department of Electrical and Computer Engineering Naval Postgraduate School Monterey, CA 93943-5000	2
6. Prof. J. B.Knorr, Code EC/Ko Department of Electrical and Computer Engineering Naval Postgraduate School Monterey, CA 93943-5000	1
7. Library of Korea Military Academy P.O.Box 77 Kongneung-dong Dobong-gu Seoul, Korea	1
8. Seo, Yong Seok 975-17 Bangbae 2-dong Kangnam-gu Seoul, Korea	1
9. G. Lambrakakis Faidonos 36 Agios Dimitrios 172 36 Athens, Greece	1

10. Gerald F. Mikucki  
Government Electric Systems Division  
General Electric Company  
Moorestown, NJ 08057

1